ISSN: 2667-4203

ESKİŞEHİR TECHNICAL UNIVERSITY JOURNAL OF SCIENCE AND TECHNOLOGY
C– Life Sciences and Biotechnology

ESKİŞEHİR TEKNİK ÜNİVERSİTESİ BİLİM VE TEKNOLOJİ DERGİSİ
C – Yaşam Bilimleri ve Biyoteknoloji

Volume/Cilt 11 Number/Sayı 1 January / Ocak - 2022

ESKİŞEHİR TECHNICAL UNIVERSITY JOURNAL OF SCIENCE AND TECHNOLOGY
C- Life Sciences and Biotechnology
Eskişehir Teknik Üniversitesi Bilim ve Teknoloji Dergisi C – Yaşam Bilimleri ve Biyoteknoloji

Volume: 11 / Number: 1 / January - 2022

Eskişehir Technical University Journal of Science and Technology C – Life Sciences and Biotechnology (formerly Anadolu University Journal of Science and Technology C – Life Sciences and Biotechnology) is an **peer-reviewed** and **refereed international journal** by Eskişehir Technical University. Since 2010, it has been regularly published and distributed biannually and it has been published biannually and **electronically only since 2016**.

Manuscripts submitted for publication are analyzed in terms of scientific quality, ethics and research methods in terms of its compliance by the Editorial Board representatives of the relevant areas. Then, the abstracts of the appropriate articles are sent to two different referees with a well-known in scientific area. If the referees agree to review the article, full text in the framework of the privacy protocol is sent. In accordance with the decisions of referees, either directly or corrected article is published or rejected. Confidential reports of the referees in the journal archive will be retained for ten years. All post evaluation process is done electronically on the internet. Detailed instructions to authors are available in each issue of the journal.

"Anadolu Üniversitesi Bilim ve Teknoloji Dergisi C- Yaşam Bilimleri ve Biyoteknoloji (Anadolu University Journal of Science and Technology C – Life Sciences and Biotechnology)" published within Anadolu University started to be published within Eskişehir Technical University which was established due to statute law 7141, in 2018. Hence, the name of the journal is changed to "Eskişehir Teknik Üniversitesi Bilim ve Teknoloji Dergisi C- Yaşam Bilimleri ve Biyoteknoloji (Eskişehir Technical University Journal of Science and Technology C – Life Sciences and Biotechnology)".

Indexed by **DOAJ** - Directory of Open Access Journals, **EBSCO** and **ULAKBIM**

ISSN: 2667-4203

ESKİŞEHİR TECHNICAL UNIVERSITY JOURNAL OF SCIENCE AND TECHNOLOGY
C- Life Sciences and Biotechnology
Eskişehir Teknik Üniversitesi Bilim ve Teknoloji Dergisi C – Yaşam Bilimleri ve Biyoteknoloji

Volume: 11 / Number: 1 / January – 2022

Owner / Publisher: Prof. Dr. Tuncay DÖĞEROĞLU for Eskişehir Technical University

CONTACT INFORMATION
Eskişehir Technical University Journal of Science and Technology
Eskişehir Technical University, Institute of Graduate Programs, 26470 Eskişehir, TURKEY
Phone: +90-222-321 35 50 /**ext.:** 1767
Fax: +90-222 335 41 22
e-mail : btdc@eskisehir.edu.tr

ESKİŞEHİR TECHNICAL UNIVERSITY JOURNAL OF SCIENCE AND TECHNOLOGY
C- Life Sciences and Biotechnology
Eskişehir Teknik Üniversitesi Bilim ve Teknoloji Dergisi C – Yaşam Bilimleri ve Biyoteknoloji

Volume: 11 / Number: 1 / January – 2022

ABOUT

Eskişehir Technical University Journal of Science and Technology C- Life Sciences and Biotechnology (formerly Anadolu University Journal of Science and Technology C - Life Sciences and Biotechnology) is an peer-reviewed and refereed international journal by Eskişehir Technical University. Since 2010, it has been regularly published and distributed biannually and it has been published biannually and electronically only since 2016.

- **The journal accepts TURKISH and ENGLISH manuscripts.**
- **The journal is indexed by EBSCO, DOAJ and ULAKBIM.**

AIM AND SCOPE

The journal publishes research papers, reviews and technical notes in the fields of theoretical sciences such as Physics, Biology, Mathematics, Statistics, Chemistry and Chemical Engineering, Environmental Sciences and Engineering, Civil Engineering, Electrical and Electronical Engineering, Computer Science and Informatics, Materials Science and Engineering, Mechanical Engineering, Mining Engineering, Industrial Engineering, Aeronautics and Astronautics, Health Sciences, Pharmaceutical Sciences, and so on.

PEER REVIEW PROCESS

Manuscripts are first reviewed by the editorial board in terms of its its journal's style rules scientific content, ethics and methodological approach. If found appropriate, the manuscript is then send to at least two referees by editor. The decision in line with the referees may be an acceptance, a rejection or an invitation to revise and resubmit. Confidential review reports from the referees will be kept in archive. All submission process manage through the online submission systems.

OPEN ACCESS POLICY

This journal provides immediate open access to its content on the principle that making research freely available to the public supports a greater global exchange of knowledge.

The journal doesn't have Article Processing Charge (APC) or any submission charges.

ETHICAL RULES

You can reach the Ethical Rules in our journal in full detail from the link below:
https://dergipark.org.tr/tr/pub/estubtdc/policy

AUTHOR GUIDELINES

All manuscripts must be submitted electronically.
You will be guided stepwise through the creation and uploading of the various files. There are no page charges. Papers are accepted for publication on the understanding that they have not been published and are not going to be considered for publication elsewhere. Authors should certify that neither the manuscript nor its main contents have already been published or submitted for publication in another journal. We ask a signed **Copyright Form** to start the evaluation process. After a manuscript has been submitted, it is not possible for authors to be added or removed or for the order of authors to be changed. If authors do so, their submission will be cancelled.

Manuscripts may be rejected without peer review by the editor-in-chief if they do not comply with the instructions to authors or if they are beyond the scope of the journal. After a manuscript has been accepted for publication, i.e. after referee-recommended revisions are complete, the author will not be permitted to make any changes that constitute departures from the manuscript that was accepted by the editor. Before publication, the galley proofs are always sent to the authors for corrections. Mistakes or omissions that occur due to some negligence on our part during final printing will be rectified in an errata section in a later issue.

This does not include those errors left uncorrected by the author in the galley proof. The use of someone else's ideas or words in their original form or slightly changed without a proper citation is considered plagiarism and will not be tolerated. Even if a citation is given, if quotation marks are not placed around words taken directly from another author's work, the author is still guilty of plagiarism. All manuscripts received are submitted to iThenticateR, a plagiarism checking system, which compares the content of the manuscript with a vast database of web pages and academic publications. Manuscripts judged to be plagiarised or self-plagiarised, based on the iThenticateR report or any other source of information, will not be considered for publication.

Preparation of Manuscript

Style and Format: Manuscripts should be **single column** by giving one-spaced with 2.5-cm margins on all sides of the page, in Times New Roman font (font size 11). Every page of the manuscript, including the title page, references, tables, etc., should be numbered. All copies of the manuscript should also have line numbers starting with 1 on each consecutive page.

Manuscripts must be upload as word document (*.doc, *.docx vb.). Please avoid uploading ***texts in *.pdf format.***

Manuscripts should be written in Turkish or English.

Symbols, Units and Abbreviations: Standard abbreviations and units should be used; SI units are recommended. Abbreviations should be defined at first appearance, and their use in the title and abstract should be avoided. Generic names of chemicals should be used. Genus and species names should be typed in italic or, if this is not available, underlined.

Please refer to equations with capitalisation and unabbreviated (e.g., as given in Equation (1)).

Manuscript Content: Articles should be divided into logically ordered and numbered sections. Principal sections should be numbered consecutively with Arabic numerals (1. Introduction, 2.

Formulation of problem, etc.) and subsections should be numbered 1.1., 1.2., etc. Do not number the Acknowledgements or References sections. The text of articles should be, if possible, divided into the following sections: Introduction, Materials and Methods (or Experimental), Results, Discussion, and Conclusion.

Title and contact information

The first page should contain the full title in sentence case (e.g., Hybrid feature selection for text classification), the full names (last names fully capitalised) and affiliations (in English) of all authors (Department, Faculty, University, City, Country, E-mail), and the contact e-mail address for the clearly identified corresponding author.

Abstract

The abstract should provide clear information about the research and the results obtained, and should not exceed 300 words. The abstract should not contain citations and must be written in Times New Roman font with font size 9.

Keywords

Please provide 3 to 5 keywords which can be used for indexing purposes.

Introduction

The motivation or purpose of your research should appear in the "Introduction", where you state the questions you sought to answer, and then provide some of the historical basis for those questions.

Methods

Provide sufficient information to allow someone to repeat your work. A clear description of your experimental design, sampling procedures, and statistical procedures is especially important in papers describing field studies, simulations, or experiments. If you list a product (e.g., animal food, analytical device), supply the name and location of the manufacturer. Give the model number for equipment used.

Results

Results should be stated concisely and without interpretation.

Discussion

Focus on the rigorously supported aspects of your study. Carefully differentiate the results of your study from data obtained from other sources. Interpret your results, relate them to the results of previous research, and discuss the implications of your results or interpretations.

Conclusion

This should state clearly the main conclusions of the research and give a clear explanation of their importance and relevance. Summary illustrations may be included.

Acknowledgments

Acknowledgments of people, grants, funds, etc. should be placed in a separate section before the reference list. The names of funding organizations should be written in full.

Conflict of Interest Statement

The authors are obliged to present the conflict of interest statement at the end of the article after the acknowledgments section.

References

Citations in the text should be identified by numbers in square brackets. The list of references at the end of the paper should be given in order of their first appearance in the text or in alphabetical order according to the surname of the fist author. All authors should be included in reference lists unless there are 10 or more, in which case only the first 10 should be given, followed by 'et al.'. Do not use individual sets of square brackets for citation numbers that appear together, e.g., [2, 3, 5–9], not [2], [3], [5]–[9]. Do not include personal communications, unpublished data, websites, or other unpublished materials as references, although such material may be inserted (in parentheses) in the text. In the case of publications in languages other than English, the published English title should be provided if one exists, with an annotation such as "(article in Turkish with an abstract in English)". If the publication was not published with an English title, cite the original title only; do not provide a self-translation. References should be formatted as follows (please note the punctuation and capitalisation):

Journal articles

Journal titles should be abbreviated according to ISI Web of Science abbreviations.

Guyon I. and Elisseeff A. An introduction to variable and feature selection. J. Mach. Learn. Res. 2003; 3: 1157-1182.

Izadpanahi S., Ozcınar C., Anbarjafari G. and Demirel H. Resolution enhancement of video sequences by using discrete wavelet transform and illumination compensation. Turk J. Elec. Eng. & Comp. Sci. 2012; 20: 1268-1276.

Books

Haupt R.L. and Haupt S.E. Practical Genetic Algorithms. 2nd ed. New York, NY, USA: Wiley, 2004.

Kennedy J. and Eberhart R. Swarm Intelligence. San Diego, CA, USA: Academic Press, 2001.

Chapters in boks

Poore JH, Lin L, Eschbach R and Bauer T. Automated statistical testing for embedded systems. In: Zander J, Schieferdecker I, Mosterman PJ, editors. Model-Based Testing for Embedded Systems. Boca Raton, FL, USA: CRC Press, 2012. pp. 111-146.

Conference proceedings

Li R.T.H. and Chung S.H. Digital boundary controller for single-phase grid-connected CSI. In: IEEE 2008 Power Electronics Specialists Conference; 15–19 June 2008; Rhodes, Greece. New York, NY, USA: IEEE. pp. 4562-4568.

Theses

Boynukalın Z. Emotion analysis of Turkish texts by using machine learning methods. MSc, Middle East Technical University, Ankara, Turkey, 2012.

Tables and Figures
All illustrations (photographs, drawings, graphs, etc.), not including tables, must be labelled "Figure." Figures must be submitted in the manuscript.

All tables and figures must have a caption and/or legend and be numbered (e.g., Table 1, Figure 2), unless there is only one table or figure, in which case it should be labelled "Table" or "Figure" with no numbering. Captions must be written in sentence case (e.g., Macroscopic appearance of the samples.). The font used in the figures should be Times New Roman with 9 pt. If symbols such as ×, μ, η, or ν are used, they should be added using the Symbols menu of Word.

All tables and figures must be numbered consecutively as they are referred to in the text. Please refer to tables and figures with capitalisation and unabbreviated (e.g., "As shown in Figure 2…", and not "Fig. 2" or "figure 2").

The resolution of images should not be less than 118 pixels/cm when width is set to 16 cm. Images must be scanned at 1200 dpi resolution and submitted in jpeg or tiff format. Graphs and diagrams must be drawn with a line weight between 0.5 and 1 point. Graphs and diagrams with a line weight of less than 0.5 point or more than 1 point are not accepted. Scanned or photocopied graphs and diagrams are not accepted.

Figures that are charts, diagrams, or drawings must be submitted in a modifiable format, i.e. our graphics personnel should be able to modify them. Therefore, if the program with which the figure is drawn has a "save as" option, it must be saved as *.ai or *.pdf. If the "save as" option does not include these extensions, the figure must be copied and pasted into a blank Microsoft Word document as an editable object. It must not be pasted as an image file (tiff, jpeg, or eps) unless it is a photograph.

Tables and figures, including caption, title, column heads, and footnotes, must not exceed 16 × 20 cm and should be no smaller than 8 cm in width. For all tables, please use Word's "Create Table" feature, with no tabbed text or tables created with spaces and drawn lines. Please do not duplicate information that is already presented in the figures.

ESKİŞEHİR TECHNICAL UNIVERSITY JOURNAL OF SCIENCE AND TECHNOLOGY
C- Life Sciences and Biotechnology
ESKİŞEHİR TEKNİK ÜNİVERSİTESİ BİLİM VE TEKNOLOJİ DERGİSİ
C– Yaşam Bilimleri ve Biyoteknoloji

Volume/ Cilt**: 11 / Number/**Sayı**: 1 / January /** Ocak **- 2022**

CONTENTS / İÇİNDEKİLER

Sayfa / Page

ESKİŞEHİR TEKNİK ÜNİVERSİTESİ BİLİM VE TEKNOLOJİ DERGİSİ C- YAŞAM BİLİMLERİ VE BİYOTEKNOLOJİ

Eskişehir Technical University Journal of Science and Technology C- Life Sciences and Biotechnology

2022, 11(1), pp. 1-10, DOI: 10.18038/aubtdc.866279

RESEARCH ARTICLE

ANTI-miRNA IMMOBILIZATION OPTIMIZATION ON THE SCREEN PRINTED ELECTRODES FOR ELECTROCHEMICAL miRNA BIOSENSORS

Karima SAHTANI [1], Yakup AYKUT [1, 2] *, Nilay ALADAG TANIK [1]

[1] Bursa Uludag University, Graduate School of Natural and Applied Sciences, Nilufer, Bursa, Turkey, 16059
[2] Bursa Uludag University, Engineering Faculty, Textile Engineering Department, Nilufer, Bursa, Turkey, 16059

ABSTRACT

Synthetically produced miRNA molecules plays an important role as biomarker to examine and investigate the diagnosis of some diseases including cancer. In order to develop a sensitive electrochemical biosensor system for the detection of miRNA molecules, the anti-miRNA molecules are synthesized and immobilized on the biosensor surfaces and observe the signal changes via a proper measurement. Immobilization time and temperature along with the anti-miRNA concentration are critically important for an appropriate observation of the miRNA detection sensitivity of the prepared biosensor system. In this regard, synthetically produced anti-miRNA **(**anti-miR451(G)**)** was purchased and diluted into different concentration by using phosphate buffer solution. Then, the solutions were immobilized on the screen printed electrodes (SPEs) and the guanine oxidation signal of the anti-miRNA molecules were observed via differential pulse voltammetry method (DPV). An appropriate concentration of the solution was selected and dropped on the SPEs and held on at different temperatures (-18, +5 and +25 ºC) for 1, 3, 14 and 21 days and DPV measurements were conducted to investigate the optimum immobilization time and temperature. The result shown that guanine oxidation signal was increased by increasing the concentration of the genetic molecules in the immobilization solution and increased less after that point when the concentration increased more because the surface reached to a certain saturation value . The guanine oxidation signal revealed that the best suitable storing temperature after the immobilization was +5 ºC determined.

Keywords: miRNA detection, Screen printed electrode, DPV measurement, Guanine oxidation

1. INTRODUCTION

Early diagnosis of diseases is important for determining an effective treatment program. Diagnosis of many diseases can be achieved by detecting and examining genetic molecules. For this, the genetic molecule can be obtained directly from the living creature that has caught the disease, or can be obtained and examined from the microorganism that causes the disease. For example, some diseases such as breast cancer[1], haemophilia A [2] and cystic fibrosis [3] are related with the human genome and could be diagnosed via genetic methods. Covid-19 [4] and influenza [5] are virus related diseases and could be diagnosed by extracting the genetic molecules from the infecting virus and investigating them by using genetic characterization methods.

The proper detection of genetics base sequences in human, viral and bacterial nucleic acids is very important in a wide range of fields, it include the detection of diseases-causing, food-contamination and a large type of pathogenic diseases. A convenient and efficient diagnostic system should be developed with caring the same level of sensitivity, precision with the ability of detecting different targets, in view of the most used diagnostic methods are laborious, time consuming and complicated. The properties of selectivity, compatibility with micro-scale technologies and the label-free characteristic make electrochemical biosensors a wide opted tool for the large applications [7]. A variety of immobilization strategies and transducing materials have been developed [6].

*Corresponding Author: aykut@uludag.edu.tr
Received: 21.01.2021 Published: 19.01.2022

Screen printing microfabrication technology is continuously in development and have been combined with the electrochemical DNA biosensors research to fabricate analyte specific sensors [8][9], the screen printed electrodes SPE proved a ductility and flexibility to be designed with a wide range of materials and able to be modified with a different biological elements such enzymes, antibodies, DNA and other recognition elements [10]. Nanomaterials have also accelerated the performance of the electrochemical application by a high bio-compatibility and enhancing the electron transfer [11], and the combination with the SPE properties could lead to a synergistic effect eliciting unforeseen advantages. As presented in the literature studies, there is a wide range of conventional electrodes, the carbon based screen printed electrodes have shown a good extent in comparison to other metals based electrodes, it was also demonstrated that there is a function between the surface morphology and the electrochemical activity of the electrodes which makes the choice of the working electrode depending upon the electroanalytical application and technique used [8].

MicroRNAs (miRNAs) are single stranded, non-coding RNA molecules established of a class of 18-22 endogenous nucleotides in length that affect the mRNA stability and translation, combining with the 3′ end of the untranslated regions (3′UTR) of target mRNAs, resulting in target gene degradation or inhibition of its translation [12]. MicroRNA play a crucial role in tumor proliferation, tumor development is associated to the glucose metabolism [13] and are predicted to regulate the expression of approximately the one-third of the human genes [14]. The literature present a wide scale of studies and have shown that some miRNA regulate cellular differentiation, proliferation and apoptotic processes, that are proved with a higher importance in cancer aggravation, the miRNA profiling across different human cancers has proved that miRNAs were an efficient indicators of the developmental origin of cancers [15].various technologies for detecting miRNA have been developed such template repairing-PCR [16], microarrays [17] and northern blotting [18], the disadvantages of these processes are the high cost and production time which is long, this make the research in continuous development to conceive a low cost, flexible and easy techniques for miRNA analysis without losing the efficiency and the level of sensitivity. miRNA-451 exists in the human genome and has been considered as biomarker for some types of cancers [19] [20]. The recent studies in this field concentrate the effort on the properties of the miRNA-451 and shown that it can modulate process of tumorigenesis and the behaviour of cancers cells by deleting a series of oncogenes [21].

Electrochemical genetic sensors are considered as an alternative way for the detection of miRNA biomarkers and have promising feature in the miRNA biosensor field because of their fast, repeatable, feasible and easy applying properties. Various electrodes such as glassy carbon electrodes[22], pencil graphite electrodes[23], screen printed electrodes[24] and carbon paste electrodes[25] are used in electrochemical genetic biosensor measurements. During the sample preparation and the measurement, first the genetic molecules were attached on the electrode surfaces and the electrochemical measurements were carried out by using a proper buffer solution. The determination of the minimum amount of the genetic molecules that are attached on the electrode surface is important to obtain an interpretable signal with a proper sensitivity. Additionally, the time between sample preparation and measurement is also another critical parameter for a correct measurement. SPEs have been widely used for the detection of miRNA molecules [24, 26].

In this study, different concentrations of the miRNA molecules were immobilized on the SPEs and the guanine oxidation signals were observed from these electrodes via differential pulse voltammetry method. Synthetic anti-miRNA molecules **(**antimiR451 (G)**)** were purchased and diluted with phosphate buffer solution. Effect of the time and temperatures were also investigated by keeping the samples at -18, +5 and +25 ^{o}C for 1, 3, 14 and 21 days and conducting measurement with these samples.

2. Material and Methods

2.1. Chemicals

All the buffer solutions used in the electrochemical measurements were prepared by using ultra-*pure water* (DNase and RNase free). The prepared solutions were kept in the sterilized glass bottles at +4 ºC until they are used. *Potassium phosphate monobasic* (KH_2PO_4), *Sodium hydroxide* (NaOH), Hydrochloric acid (HCl) and glacial acetic acid were purchased from Sigma Aldrich. Potassium phosphate dibasic (HK_2O_4P) was purchased from Scharlau. Anti-miRNA (**polyT-antimiR451(G),** 28mer DNA, Scale M inclusive HPLC) molecules used in this study were received from Genaxxon Bioscience (Germany). The sequence of the oligonucleotide is given as following: *5'-TTT TTT AAC TCA GTA ATG GTA ACG GTT T-3'*

2.2. Preparation of Phosphate Buffer Solution (PBS)

0.05 M PBS solution was prepared with 1.36 gr (0.01 mol) KH_2PO_4 and 6.96 gr (0.04 mol) HK_2O_4P by dissolving them in 1 lt ultra-*pure* water. In order to bring the solution to pH 7.4 NaOH or HCl was added into the solution. Finally, 1.168 gr NaCl was put into the prepared solution to adjust the NaCl as 0.02 M in the solution.

2.3. Preparation of Acetate Buffer Solution (ABS)

0.5 M ABS solution was prepared by setting 0.5 M glacial acetic acid in 500 ml ultra-pure water. NaOH or HCl was added into the solution in order to bring the solution to pH 4.8. Finally, 1.168 gr NaCl was put into the prepared solution to adjust the NaCl as 0.02 M in the solution.

2.4. Preparation of Anti-miRNA Stock and Measurement Solutions

Anti-miRNA stock solution was prepared as 1000 ppm. The purchased anti-miRNA was firstly dissolved in ultra-pure water for stock solution preparation. The stock solution was poured in the PCR tubes as 50 µl and stored at -18 ºC until they are going to be used. The measurement anti-miRNA solutions were prepared by diluting the stock solutions. Stock solutions were shared into empty PCR tubes as 10 µl, and then 50 µl of PBS was added into the PCR tubes for the dilution. A vortex mixture was used for the stock and measurement solution preparations.

2.5. Attachment of Anti-miRNA Molecules on SPEs Surfaces

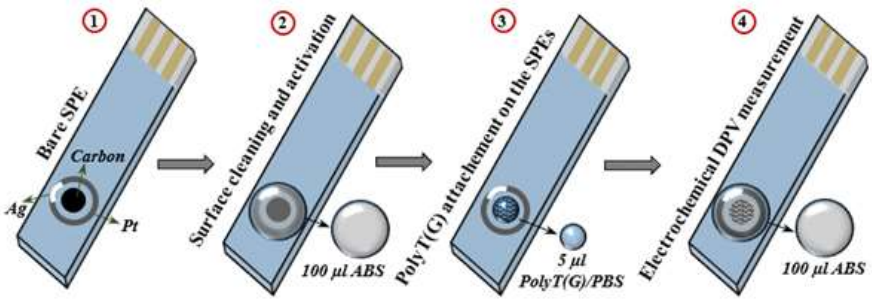

Figure 1. Surface cleaning and activation, anti-miRNA attachment and measurement process.

Surface cleaning and activation of the SPEs were carried out electrochemically with DPV method before the immobilization of anti-miRNA molecules. All the process steps were schematically illustrated in Figure 1. This process was conducted by dropping 100 µl of ABS on the electrode surface and applying

1.4 deposition potential for 60 s with 600 estimated number of the points and flowingly apply potential between 0.7-1.4 V with 10 mV/s scanning rate. After the cleaning and activation process, the surface of the SPEs were washed by dropping 300 µl PBS with a micropipette and left them to dry until they are going to be used. The attachment of the anti-miRNA molecules on the SPEs were carried out by dropping the measurement solution on the surfaces. 5 µl of anti-miRNA measurement solution was dropped on the previously cleaned and activated SPEs and waited for 1 hr. Then, electrode parts of the SPEs surfaces were washed with 300 µl of PBS before the measurement in order to remove unattached anti-miRNA molecules on SPEs. After the PBS washing, the sample surfaces were dried for 1 hr before the measurement.

2.6. Electrochemical Measurements of the Biosensory System via DPV Measurements

Electrochemical measurements were performed by using Potansiyostat - AUTOLAB AUT204 (Eco Chemie, Nederland) and NOVA 1.11 software. Screen-printed electrodes (SPEs) were purchased from *Metrohm* with DS 150 product code which has carbon working electrode, platinum auxiliary electrode (PAE) and silver reference electrode. DS 110 product code model which differently has carbon auxiliary electrode (CAE) was also tried in the initial measurements. Photograph images of the SPEs during anti-miRNA immobilization and DPV measurement were shown in Figure 2. The measurements were carried out between 0.75-1.3 V with 10 mV/s scanning rate by dropping 100 µl ABS on the electrode surface.

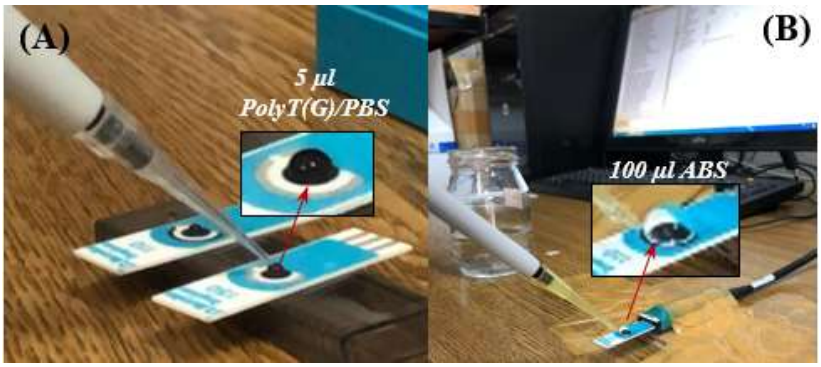

Figure 2. (A) Measurement anti-miRNA solution drop on the working electrode of SPE and (B) ABS solution drop on SPE during the measurement.

3. RESULTS AND DISCUSSION

3.1. DPV Measurement by using PBS Buffer Solution

PBS and ABS as two different buffer solutions were prepared in order to observe which buffer solution is better for an appropriate DPV measurement. It was begun with PBS solution at the measurements. In this regard, two different ways have been tried. First, the prepared measurement solution (anti-miRNA/PBS) was directly dropped on the SPE and the DPV measurement was conducted (Figure 3a and 3c). In the second way, the measurement solution was dropped on the SPE, waited for 60 min and then washed with just PBS the remove unattached molecules and DPV measurement was carried out (Figure 3b and 3d). These two methods were examined by using two different SPE types which has either platinum (Figure 3a and 3b) or carbon (Figure 3c and 3d) auxiliary electrode. Both guanine and adenine oxidation peaks were appeared at all the measurements when the plots were observed as given in Figure 3. When the results were compared with the literature, these peaks are generally appeared around 1 and 1.25 V correspond to guanine and adenine oxidations [27,28]. These peaks seems shifted to lower voltage values when the measurements were conducted by using PBS solution. In order to

observe the effect clearly with PBS measurement, ABS cleaning and activation was not applied to the SPEs in this group of the measurement before the anti-miRNA attachment and the measurement.

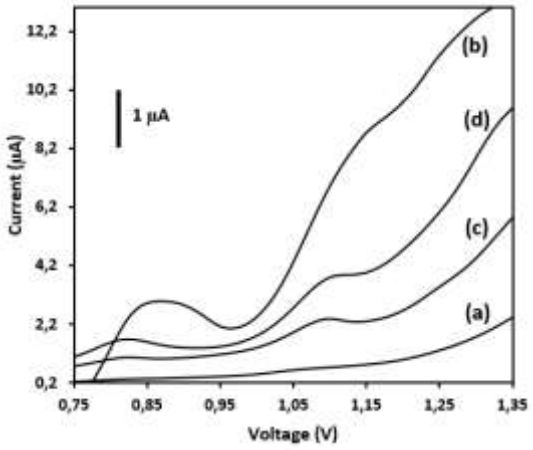

Figure 3. DPV measurement with PBS: (a) anti-miRNA/PBS (with PAE), (b) anti-miRNA/PBS wait 60 min-wash –measure (with PAE), (c) anti-miRNA/PBS (with CAE) and (d) anti-miRNA/PBS wait 60 min-wash – measure (with CAE).

3.2. DPV Measurement by using ABS Buffer Solution

ABS solution was also used during the DPV measurement, since when PBS solution was used the guanine and oxidation peak positions were not matched as in the studies published literature. Metrohm with DS 150 product code SPEs were used at all the measurements when ABS was used. In the measurement, 5 µl of anti-miRNA measurement solution was dropped on the previously cleaned and activated SPEs and waited for 1 hr. Then the samples were washed with PBS, dried and the measurement was carried out by putting 100 µl of ABS solution during the measurement. When the measurement plot was observed (obtained) as in Figure 4, it was observed that guanine and adenine oxidation peaks positions were matching as in the literature [27,28]. After the comparison of the results of PBS and ABS measurements with the literature, since the results were compatible when ABS was used as the buffer solution for the measurement, all the measurements were continued by using ABS solution.

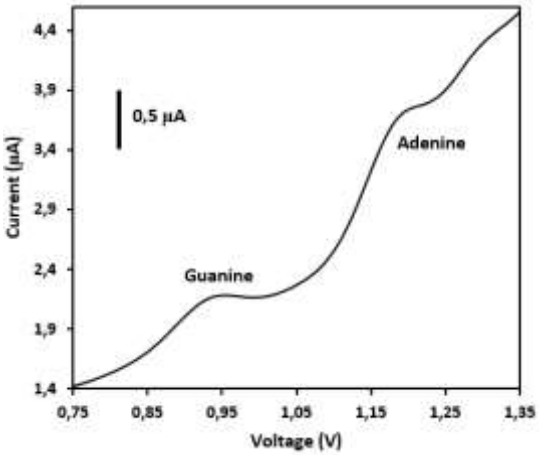

Figure 4. DPV measurement with ABS buffer solution.

3.3. DPV Measurement with Different Rate of Anti-miRNA Attached SPEs

The effect of the anti-miRNA concentration in the measurement solutions was studied by preparing five different diluting concentrations. The dilution was carried out by adjusting the anti-miRNA measurement solution/PBS (v/v) rate a 1/50, 2/50, 5/50, 10/50 and 20/50. Then, the prepared diluted solutions were dropped on the previously surface cleaned and activated SPEs, waited 1 hr, washed with PBS, dried for 1 hr and then the measurements were conducted. As seen from Figure 5, guanine and adenine oxidation peaks were clearly detected around 1 and 1.25 V sequentially [27,28]. The intensity of the guanine oxidation peak dramatically increased when the ratio of the anti-miRNA molecules were increased in the measurement solution up to 10/50 anti-miRNA measurement solution/PBS rate, and was not increased dramatically while increasing anti-miRNA ratio in the solution. On the other hand, there was a prominent enhancement at the adenine oxidation peak when the anti-miRNA measurement solution/PBS rate increased from 2/50 to 5/50, and not significant changes were observed at other concentrations. The results revealed that guanine and adenine oxidation peaks are detectable at every concentration, so the minimum concentration can be used in the following studies.

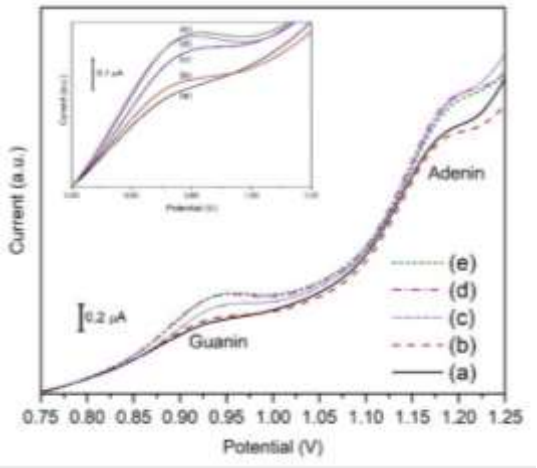

Figure 5. DPV measurement with different rate of anti-miRNA attached SPEs: anti-miRNA measurement solution/PBS (v/v) rates are (a) 1/50, (b) 2/50, (c) 5/50, (d) 10/50 and (e) 20/50.

3.4. Storage Time and Temperature Study of anti-miRNA Attached SPEs

In order to investigate the appropriate time and temperature of the anti-miRNA immobilized SPEs, DPV measurements were carried out after the samples stored at -18, +5 and +25 ^{o}C for 1, 3, 14 and 21 days. The DPV measurements plots were demonstrated in Figure 6. When it was focused on the guanine oxidation signal around 0.9-1.0 V, there was a dramatic decrease at the -18 ^{o}C stored sample when the measurement was conducted after one day stored samples. On the other hand, no significant change was observed at +5 ve +25 ^{o}C stored samples. The measured oxidation signal was always lower at -18 and +25 ^{o}C stored sample than +5 ^{o}C stored sample. Overall results revealed that the most suitable storage temperature after anti-miRNA attached samples until the measurement was +5 ^{o}C.

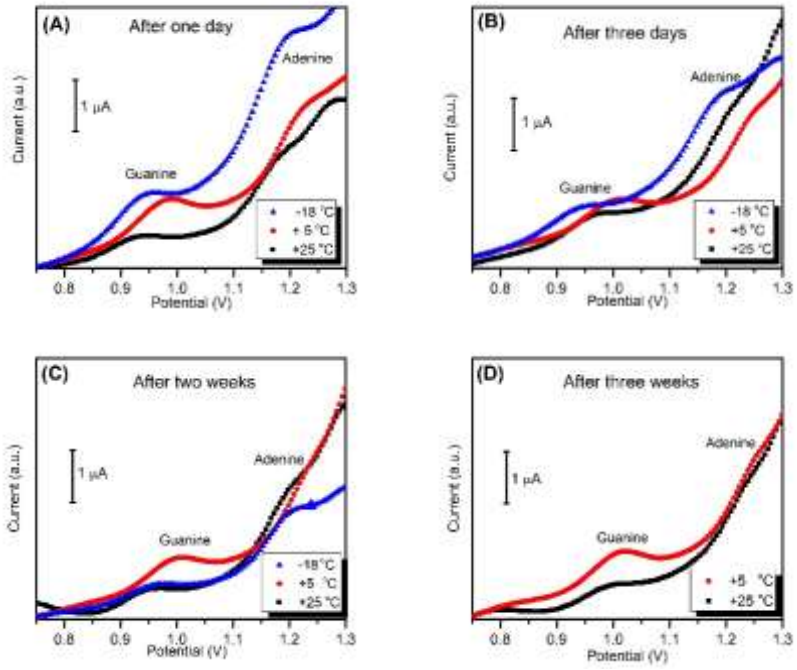

Figure 6. DPV measurements of anti-miRNA attached SPEs at different storage times at -18, +5 and +25 ºC stored samples: (A) 1 day, (B) 3 days, (C) 14 days and (D) 21 days.

4. CONCLUSION

Anti-miRNA immobilization optimization on the screen-printed electrodes for the sensitive detection of miRNA molecules were carried out. In this regard, different amounts of anti-miRNA molecules were attached on SPE surfaces and guanine oxidation signals were electrochemically measured and analysed in order to determine the best adequate immobilization concentration. Additionally, time and temperature after the anti-miRNA attachments on the SPEs were also investigated. The same amount of anti-miRNA molecules was immobilized on the SPEs and stored in -18, +5 and +25 ºC for 1, 3, 14 and 21 days. Then, guanine oxidation signals were observed again to determine the best time and temperature. The results demonstrated that even though the guanine oxidation signal dramatically increased by increasing anti-miRNA content in the immobilization solution, the signal was not increased more when it was continued to increase anti-miRNA content. Time and temperature result revealed that the best suitable condition was +5 ºC since the guanine oxidation signal intensity decrease less with time and was more stable comparing the other sample groups.

ACKNOWLEDGEMENT

The present study was part of a research project funded by The Scientific & Technological Research Council of Turkey (TUBITAK, Project no. 118M231). The study is a part of Karima Sahtani's PhD thesis work in the Graduate School of Natural and Applied Sciences at Bursa Uludag University.

CONFLICT OF INTEREST

The authors stated that there are no conflicts of interest regarding the publication of this article.

REFERENCES

[1] Wooster R, Weber BL. Breast and ovarian cancer. N Engl J Med, 2003; 348: 2339-2347.

[2] Rezaei H, Motovali-bashi M, Radfar S. An enzyme-free electrochemical biosensor for simultaneous detection of two hemophilia A biomarkers: Combining target recycling with quantum dots-encapsulated metal-organic frameworks for signal amplification. Anal Chim Acta, 2019; 1092: 66-74.

[3] Dequeker E, Stuhrmann M, Morris M.A., Casals T., Castellani C, Claustres M, Cuppens H, des Georges M, Ferec C., Macek M, Pignatti PF., Scheffer H, Schwartz M., Witt M, Schwarz M, Girodon, E. Best practice guidelines for molecular genetic diagnosis of cystic fibrosis and CFTR-related disorders - Updated European recommendations. Eur J Hum Genet, 2009; 17: 51–65.

[4] Chan JF, Yip CC, To KK, Tang TH, Wong SC, Leung KH, Fung AY, Ng AC, Zou, Z, Tsoi HW, Choi GK, Tam, AR, Cheng VC, Chan KH, Tsang OT. Yuen KY. Improved molecular diagnosis of COVID-19 by the novel, highly sensitive and specific COVID-19-RdRp/Hel real-time reverse transcription-polymerase chain reaction assay validated in vitro and with clinical specimens . J Clin Microbiol, 2020; 58: e00310-20.

[5] Van TT, Miller J, Warshauer DM, Reisdorf E, Jernigan D, Humes R, Shult PA. Pooling nasopharyngeal/throat swab specimens to increase testing capacity for influenza viruses by PCR. J Clin Microbiol, 2012; 50: 891-896.

[6] Carpini G, Lucarelli F, Marrazza G, Mascini M. Oligonucleotide-modified screen-printed gold electrodes for enzyme-amplified sensing of nucleic acids. Biosens Bioelectron, 2004; 20: 167-175.

[7] Malecka K, Stachyra A, Góra-Sochacka A, Sirko A, Zagórski-Ostoja W, Radecka H, Radecki J. Electrochemical genosensor based on disc and screen printed gold electrodes for detection of specific DNA and RNA sequences derived from Avian Influenza Virus H5N1. Sensors Actuators B Chem, 2016; 224: 290-297.

[8] Fanjul-Bolado P, Hernández-Santos D, Lamas-Ardisana PJ, Martín-Pernía A, Costa-García A. Electrochemical characterization of screen-printed and conventional carbon paste electrodes. Electrochim Acta, 2008; 53: 3635–3642.

[9] Kondo T, Sakamoto H, Kato T, Horitani M, Shitanda I, Itagaki M, Yuasa M. Screen-printed diamond electrode: A disposable sensitive electrochemical electrode. Electrochem Commun, 2011; 13: 1546-1549.

[10] Arduini F, Micheli L, Moscone D, Palleschi G, Piermarini S, Ricci F, Volpe G. Electrochemical biosensors based on nanomodified screen-printed electrodes: Recent applications in clinical analysis. Trends Anal Chem, 2016; 79: 114-126.

[11] Das R, Sharma MK, Rao VK, Bhattacharya BK, Garg I, Venkatesh V, Upadhyay S. An electrochemical genosensor for Salmonella typhi on gold nanoparticles-mercaptosilane modified screen printed electrode. J Biotechnol, 2014; 188, 9-16.

[12] Kloosterman WP, Plasterk RH. The Diverse Functions of MicroRNAs in Animal Development and Disease. Dev Cell, 2006; 11: 441-450.

[13] Guo H, Nan Y, Zhen Y, Zhang Y, Guo L, Yu K, Huang Q, Zhong Y. miRNA-451 inhibits glioma cell proliferation and invasion by downregulating glucose transporter 1. Tumor Biol, 2016; 37: 13751–13761.

[14] Gartel AL, Kandel ES. miRNAs: Little known mediators of oncogenesis. Semin Cancer Biol, 2008; 18: 103-110.

[15] Wang XC, Tian LL, Jiang XY, Wang YY, Li DG, She Y, Chang JH., Meng AM. The expression and function of miRNA-451 in non-small cell lung cancer. Cancer Lett, 2011; 311: 203–209.

[16] Zhou D, Lin X, Gao W, Piao J, Li S, He N, Qian Z, Zhao M, Gong X. A novel template repairing-PCR (TR-PCR) reaction platform for microRNA detection using translesional synthesis on DNA templates containing abasic sites. Chem Commun, 2019; 55: 2932-2935.

[17] Dong R, Shen Z, Zheng C, Chen G, Zheng S. Serum microRNA microarray analysis identifies miR-4429 and miR-4689 are potential diagnostic biomarkers for biliary atresia. Sci Rep, 2016; 6: 21084.

[18] Shabaninejad Z, Yousefi F, Movahedpour A, Ghasemi Y, Dokanehiifard S, Rezaei S, Aryan R, Savardashtaki A, Mirzaei H. Electrochemical-based biosensors for microRNA detection: Nanotechnology comes into view. Anal Biochem, 2019; 581: 113349.

[19] Wang H, Zhang G, Wu Z, Lu B, Yuan D, Li X, Lu Z. MicoRNA-451 is a novel tumor suppressor via targeting c-myc in head and neck squamous cell carcinomas. J Cancer Res Ther, 2015; 11: 216-221.

[20] Kovalchuk O, Filkowski J, Meservy J, Ilnytskyy Y, Tryndyak VP, Chekhun VF, Pogribny IP. Involvement of microRNA-451 in resistance of the MCF-7 breast cancer cells to chemotherapeutic drug doxorubicin. Mol Cancer Ther, 2008; 7: 2152–2159.

[21] Yuan J, Lang J, Liu C, Zhou K, Chen L, Liu Y. The expression and function of miRNA-451 in osteosarcoma. Med Oncol, 2015; 32, 1-7.

[22] Ehzari H, Amiri M, Safari M. Enzyme-free sandwich-type electrochemical immunosensor for highly sensitive prostate specific antigen based on conjugation of quantum dots and antibody on surface of modified glassy carbon electrode with core–shell magnetic metal-organic frameworks. Talanta, 2020; 210: 120641.

[23] Yammouri G, Mandli J, Mohammadi H, Amine A. Development of an electrochemical label-free biosensor for microRNA-125a detection using pencil graphite electrode modified with different carbon nanomaterials. J Electroanal Chem, 2017; 806: 75-81.

[24] Erdem A, Eksin E, Congur G. Indicator-free electrochemical biosensor for microRNA detection based on carbon nanofibers modified screen printed electrodes. J Electroanal Chem, 2015; 755: 167-173.

[25] Azab SM, Elhakim HA, Fekry A. The strategy of nanoparticles and the flavone chrysin to quantify miRNA-let 7a in zepto-molar level: Its application as tumor marker. J Mol Struct, 2019; 1196: 647-652.

[26] Ganguly A, Benson J, Papakonstantinou P. Sensitive chronocoulometric detection of miRNA at screen-printed electrodes modified by gold-decorated MoS2 nanosheets. ACS Appl Bio Mater,

2018; 1: 1184-1194.

[27] Bagni G, Hernandez S, Mascini M, Sturchio E, Boccia P, Marconi S. DNA biosensor for rapid detection of genotoxic compounds in soil samples. Sensors, 2005; 5: 394-410.

[28] Lin X, Ni Y, Pei X, Kokot S. Electrochemical detection of DNA damage induced by clenbuterol at a reduced graphene oxide-Nafion modified glassy carbon electrode. Anal Methods, 2017; 9: 1105-1111.

ESKİŞEHİR TEKNİK ÜNİVERSİTESİ BİLİM VE TEKNOLOJİ DERGİSİ C- YAŞAM BİLİMLERİ VE BİYOTEKNOLOJİ

Eskişehir Technical University Journal of Science and Technology C- Life Sciences and Biotechnology

2022, 11(1), pp.11-21, DOI: 10.18038/aubtdc.695517

RESEARCH ARTICLE

A NOVEL AND EFFICIENT PHOTOCATALYSIS (ZnO/BENTONITE) FOR DISINFECTION OF *Escherichia coli* AND *Pseudomonas aeruginosa* UNDER VISIBLE LIGHT IRRADIATION

Öge ARTAGAN [1,*], Ali İmran VAİZOĞULLAR [1]

[1] Medical Service and Techniques Department, Vocational School of Health Services, Muğla Sıtkı Koçman University, Muğla, Turkey

ABSTRACT

In the present study, a new composite catalyst which highly active under the visible light was synthesized by immobilizing onto bentonite surface using ZnO materials (ZnO/Bent). For this, a simple in situ participant technique was used. The samples were characterized using SEM, XRD, BET techniques. SEM images possess that ZnO particles have nearly a spherical structure. Bentonite clay was used to increase the surface area of the samples. The obtained BET surface area of the samples shows that the ZnO/Bent catalyst was lower than that of pure Bentonite. The aim of this study was to evaluate the effectiveness of photocatalytic disinfection with ZnO-Bent composite against *Escherichia coli* and *Pseudomonas aeruginosa* under visible light. The obtained results show that when *E. coli* strain was subjected to ZnO-Bent mediated photocatalytic disinfection under solar irradiation, more than 98 % disinfection of the targeted *E. coli* was achieved within 2 hours and also 100% of *P. aeruginosa colonies* were inactivated within 4 hours under solar irradiation. A Possible degradation mechanism for ZnO/Bent composite was proposed in this study.

Keywords: Antimicrobial Disinfection, Photocatalysis, ZnO-Bent, *Escherichia coli*, *Pseudomonas aeruginosa*

1. INTRODUCTION

Recently, toxic organic compounds that come from industrial development have caused a great environmental problem. Thus, the removal of these pollutants has become a major problem in scientific research. These organic toxic compounds negatively affect the human, environment and other organism's health in nature [1]. Every year, so many people are affected by contaminations of microorganisms (viral, bacterial) in the environment. Especially intestinal infections caused by contaminated water have also become leading causes of malnutrition and poor digestion [2]. The technology has the potential to provide an alternative method against the spread of infections, especially in view of the progress of visible light-activated catalysts. Photocatalysis has much more attention attracted worldwide due to its potential to inactivate a wide variety of microorganisms, by using solar energy. Photocatalysis is a safe, non-toxic, and rather cheap disinfection method and also adaptability allows it to be used for many purposes. Photocatalysis is a viable alternative technology for water treatment, indoor air, medical equipment disinfection, pharmaceutics, food industry, plant protection, wastewater purification systems, drinking water disinfection largely because of its potential use. Direct solar energy success both disinfection and chemical detoxification [3, 4, 5, 6]. Disinfection of microorganisms by photocatalysis is of particular importance when compared to traditional chemical applications. Chlorination and other chemical applications have so many disadvantages. For instance, using chlorine for disinfection may regenerate organics in the water to chloro-organic compounds which are quite carcinogenic [7, 8]. Another thought of the traditional disinfection method is that pathogens and their cysts tend to develop resistance to chlorine disinfection or require higher doses for complete disinfection [7-10]. Different alternatives of disinfection for instance ozonation and irradiation have

*Corresponding Author: ogebasoglan@mu.edu.tr
Received:27.02.2020 Published: 19.01.2022

some limitations, for instance, the lack of residual effect [11] and generation of colony alternatives [6, 12, 13]. Bentonite is a silicate-based clay mineral. It has a large specific surface area and great absorption property. Some researchers expressed that bentonite based ZnO is an efficient composite photocatalyst. It can have degraded organic toxins in the water medium. Also, Bentonite can effectively light absorption in the visible region. This caused more photoactive performance for ZnO/Bent photocatalysts sample [15]. There are so many studies about photocatalytic disinfection. For example, Sun and co-workes were studied the disinfections of *Aspergillus flavus.* They expressed that as synthesized composites were composed of rhombic $NiFe_2O_4$ nanosheets and g-C_3N_4 nanosized sheets, and 0.2 g-C_3N_4/$NiFe_2O_4$ (mass ratio) demonstrated the perfect activity with above 90% disinfection rate under 90 minutes visible light irradiation. The efficient disinfection performance was atributed to the supportive charges' separation, fine photoelectric properties and proper band structure [16]. Another work was performed by Najma and co-workers [17]. They stated that the structure and morphology of ZnO has an effective catalytic surface due to the hierarchical porosity and membrane formation on AAO substrates which showed a strong catalytic performance against E-coli. They also stated that the obtained results facilitated the transfer and diffusion of Zn^{2+} by the oxygen species in the reaction medium together with the large catalytic surface [17]. The study about the effective catalytic performance of zinc against some bacteria when in composite form was carried out by Karunakaran and co-workers. According to their findings, the incorporation of ZnO in TiO_2 has higher charge transfer resistance and lower capacitance under visible light [18]. The above studies have shown that photocatalytic disinfection processes can be applied by so many materials.

In the present study, ZnO and bentonite supported ZnO was synthesized by facile precipitation method. The visible light utility photocatalytic disinfection of microorganisms by ZnO/Bent composite. ZnO/Bent photocatalytic disinfection model has not been used against *E. coli* and *P. aeruginosa* until this time.

2. MATERIAL AND METHOD

All materials were of analytical grade except Bentonite, and they were used without purification. Firstly, 12.5 ml of ethylene glichol, 4,5 g of Zn $(NO_3)_2.2H_2O$ were added to 50 ml of water and stirred for 30 min at 40°C (Solution A). simultaneously, 44 ml of LiOH solution (0.1 mol/L^{-1}) was added to solution A. Cloudly like Zn $(OH)_2$ was obtained onto Bentonite surface and stirred for 3 h. Hexane was added to ZnO sol to store for a night at 5°C. the white gel and then centrifuged and rinsed with distilled water. The obtained particle was dried at 80°C and calcined at 300°C for 3 hours. Bare ZnO nano spherics were synthesized as defined above procedure without the addition of bentonite.

The crystalline phase was examined by XRD (Rigaku Dmax 350) using copper K radiation (λ =0.154056 nm). The microstructure and shape of the particle were researched using SEM (JEOL JSM-7600F). The element was determined with (JEOL JSM-7600F) EDAX analyzer with SEM measurement. The Brunauer-Emmett-Teller (BET), pore-volume, and pore size were measured using ASAP2010 (Micromeritics Instrument Corporation, USA) with N_2 adsorption at 77.35 K.

2.1. Antimicrobial Activity on Bio ball

The antimicrobial susceptibility profile of ZnO-Bent was determined by the Spreading Plate method. BioBall MultiShot 10E8 is a freeze-dried water-soluble ball containing a precise number of viable cells. BioBall is produced to the world's highest quality standards, achieving ISO Guide 34, a standard for reference material producers, accreditation. Each BioBall was rehydrated in 1.1 mL Re-Hydration Fluid containing 10 doses of 100 uL with 10^7 cfu each, resulting in a target concentration of 5×10^5 cfu per mL when inoculated in 20 mL of Nutrient Broth (NB) [13]. Activated bacteria were used in the Spreading Plate method [14].

2.2. Bacterial Strains and Growth Conditions

E. coli (NCTC 12923*), P. aeruginosa (*NCTC 12924*)* BioBall MultiShot 10E8 were used. Nutrient agar for bacteria was prepared and diluted to 25 ml of petri dishes for the purpose of studying the surviving microorganisms. The material was weighed at 250 μg/mL and incubated with microorganisms. At the 2nd, 4th and 6th hours samples were taken, incubated in daylight, specimens taken, transferred to new petri dishes and incubated for 24 hours at 37 ° C, then the colonies were counted with the help of a magnifying glass.

3. RESULTS

3.1.XRD Analysis

Figure 1 shows the XRD patterns of Bent, ZnO and ZnO-Bent materials. From Figure 1, the characteristic peak of bentonite at 21.81°, 27.62 and 35.88 2θ degrees are seen in the Bentonite structure. The peaks appear at 2θ=31.83, 34.45, 36.28, 47.56 are shown in ZnO-Bent pattern which is wurtzite structure of ZnO indexed as (1 0 0), (0 0 2), (1 01), (1 0 2) plane respectively [19]. Also, bentonite and no peaks are obtained in the ZnO-Bent XRD sample [20].

The intensity of major peaks of ZnO decreased in ZnO/Bent sample. The decrease in diffraction peaks of ZnO was related to the interaction between Bentonite and ZnO oxides. These results confirmed that ZnO dispersed onto the Bentonite surface effectively. The calculated particle size of ZnO and ZnO-Bent from the Debye-Scherer equation was obtained to be 30, 50 and 80 nm approximately.

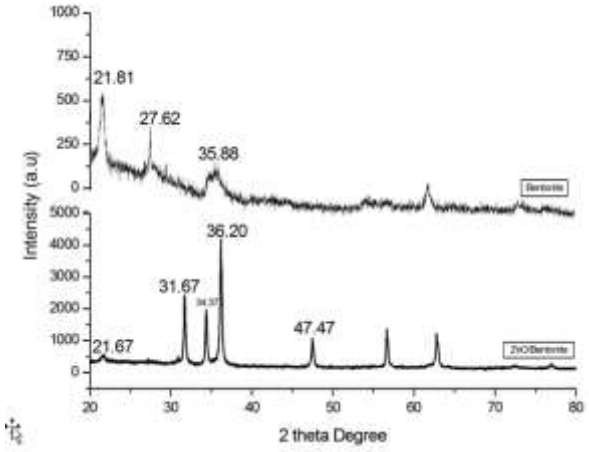

Figure1. XRD pattern of Bentonite and ZnO/Bent catalysts

3.2. SEM and BET Analysis

SEM analyses of the samples are presented in Figure 2. From Figure2, bentonite clay has cottony–like structure. ZnO particles displayed nano spherical morphology. In addition, the SEM image of the ZnO-Bentonite catalyst exhibited the same morphology with the ZnO. This indicated that bentonite clay did not change the ZnO morphology. However, the particle size of the ZnO decreased after immobilization onto the bentonite surface. This confirmed that effective dispersion caused lower particle aggregation energy. The BET surface areas of the synthesized catalysts are shown in Table 1. From table 1, as seen, the BET surface area of the ZnO-Bent sample decreased effectively confirming the excellent dispersion onto the bentonite surface.

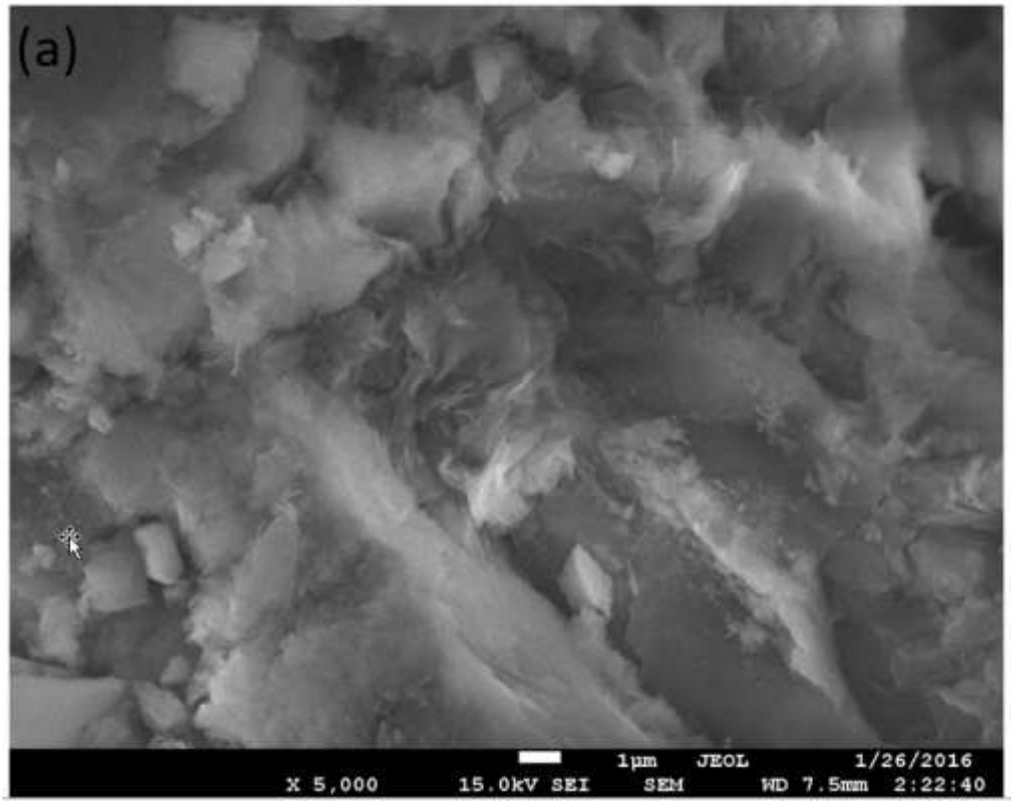
(a)
1µm JEOL 1/26/2016
X 5,000 15.0kV SEI SEM WD 7.5mm 2:22:40

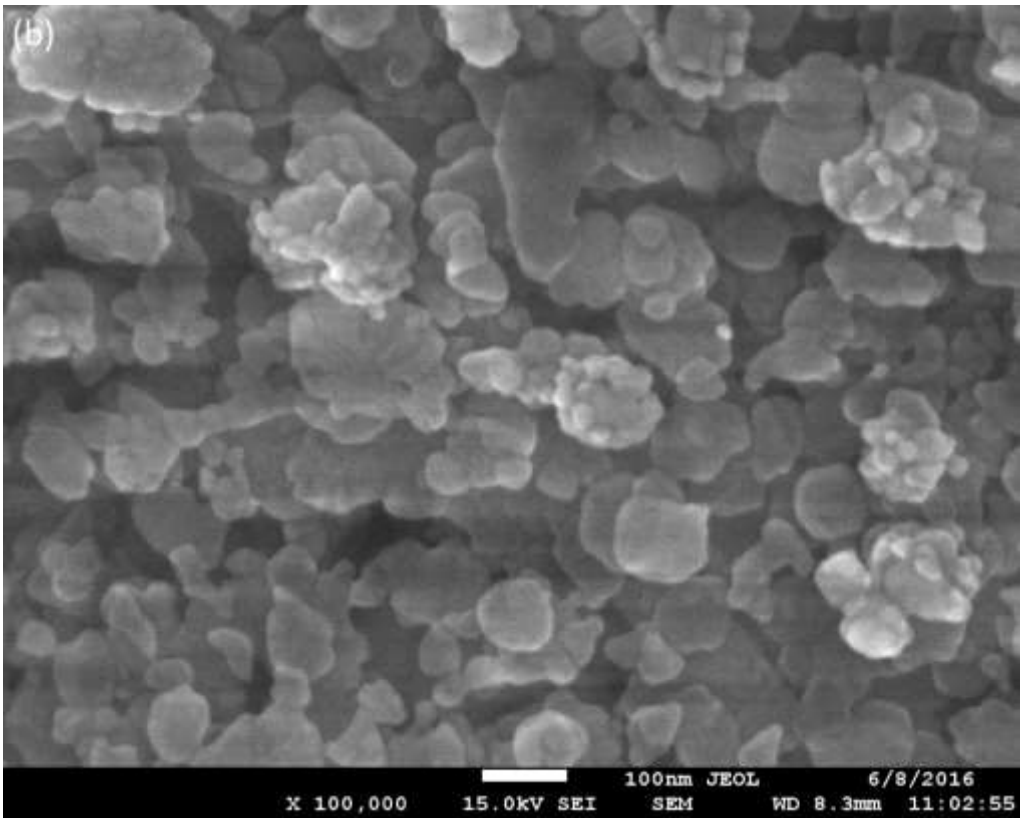
(b)
100nm JEOL 6/8/2016
X 100,000 15.0kV SEI SEM WD 8.3mm 11:02:55

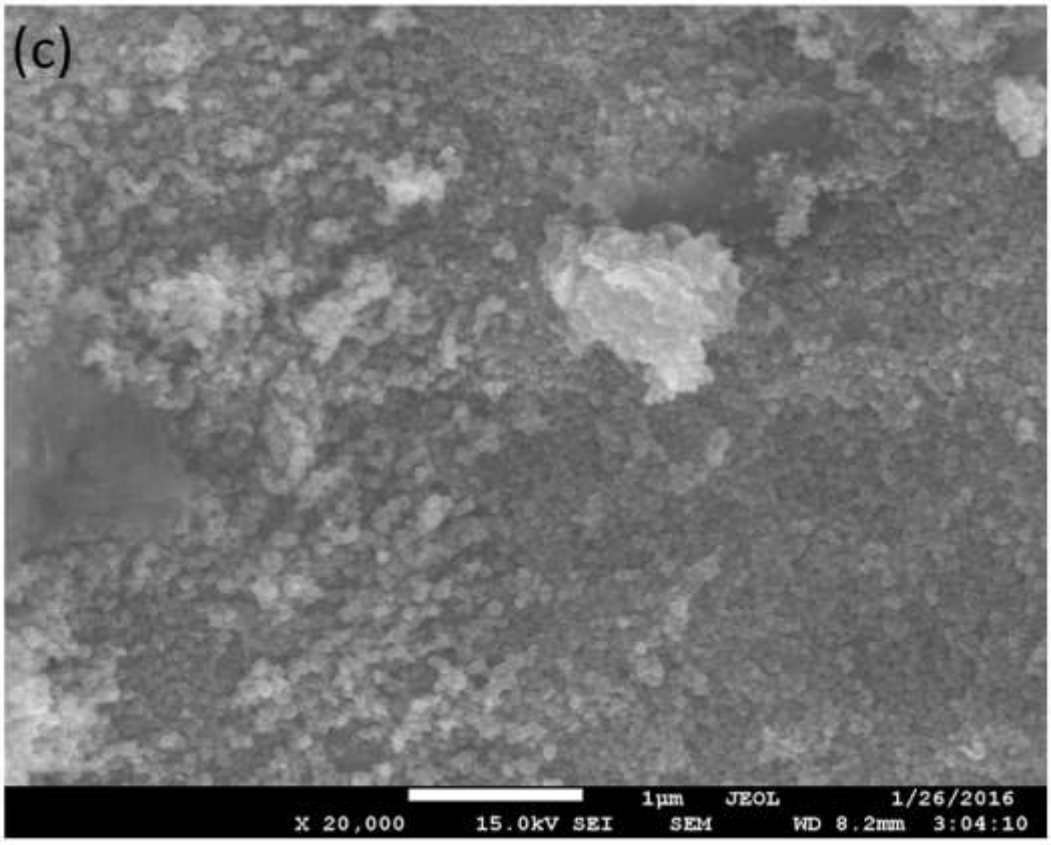

Figure 2. SEM images of Bentonite (a), ZnO (b) and ZnO/Bent (c) catalysts

Table 1. Textural and pseudo first-order data of the synthesized catalysts

Sample	BET (m^2/g)	Pore volume (cm^3/g)	Pore size (nm)
Bentonite	125.25	1.689	17.98
ZnO	2.563	0.055	1.295
ZnO-Bent	56.10	0.158	11.622

3.3. UV-DRS analysis and Structural Properties

Figure 3 presents the UV-DRS spectra of the ZnO and ZnO-Bent samples. As seen that both samples show a strong absorbance between 300-400 nm. The absorption spectrum of ZnO shifted to a higher wavelength when it was loaded onto bentonite clay. The edge of the bandgap of ZnO and ZnO/Bent are 381 and 406 nm respectively. The bandgap energy which can be calculated from the onset of the absorption edge (λ_g) using the $E_g = {}^{1240}/_{\lambda_g}$ the formula is 3.25 and 3.05 eV for the ZnO and ZnO/Bent catalysts respectively (redshift). These results are likely to be related to crystallite defects after dispersed onto the bentonite surface. This also shows that bentonite assisted ZnO (ZnO-Bent) has useful for the degradation of hazardous under visible light [21].

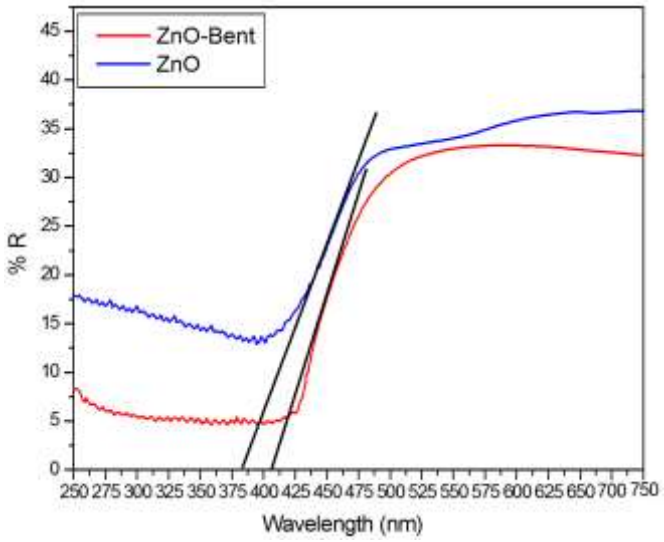

Figure 3. UV-DRS spectra of the samples

Photocatalytic mechanism has been potential of inactivation of diverse microorganisms such as bacteria (gram-positive and negative), endospores, fungi, algae, protozoa, viruses. Photocatalysis has also been shown to be capable of inactivating prions [24]. Foster and friends (2011) reported that; In recent years, there has been a significant increase in the number of publications referring to photocatalytic disinfection models [25].

Mahon and friends investigated the performance of photocatalytic treatment processes by using different photocatalysts against *E. coli* and bacteriophages MS2, ΦX174 and PR772, under real sunlight conditions [26].

Oh,and friends investigated the antibacterial activity of the CuBi2O4 composites (i.e. CuO–CuB, CuO–CuB–EG, CuO2–CuB–EG and CuO3–CuB–EG) against *E. coli*. *E. coli* (major group of Gram-negative bacteria) was selected as the model pathogenic organism [27].

The performance of the photocatalytic treatment process was assessed using ZnO-Bent photocatalysts against *E. coli* and *P. aeruginosa*. Figure 5 shows a plate with *E. coli* colonies in the initial concentration sample, as a control. Photocatalytic disinfection by ZnO- Bent against *E. coli* reached the max level within 2 hours (Figure 5-6). Within 2 hours of photocatalysis, 98.3 % (Table 3) of *E coli* inactivation was achieved and then within 4 hours of photocatalysis with daylight, 89% (detailed in table 3) of *E. coli* was inactivated (Figure 6). Figure 6 shows that there has been a sharp drop in the number of *E. coli* colonies within 2 hours of ZnO-Bent photocatalyst activity.

Figure 7 shows a plate with *P. aeruginosa* colonies in the initial concentration sample, as a control. After 2 hours of irradiation with visible light 86% of *P. aeruginosa* were inactivated. Photocatalytic disinfection by ZnO- Bent against *P. aeruginosa* reached the maximum level within 4 hours (Figure 7-8).

The antibacterial potential of ZnO-Bent under visible light irradiation was detailed in Table 3. ZnO-Bent photocatalytic activitiy was evaluated by the inactivation of *E. coli* and *P. aeruginosa*. The experimental results showed that ZnO-Bent inactivated 98.3% of *E. coli* colonies within 2 hours incubation and inactivated 100 % of *P. aeruginosa* colonies within 4 hours (Table 3).

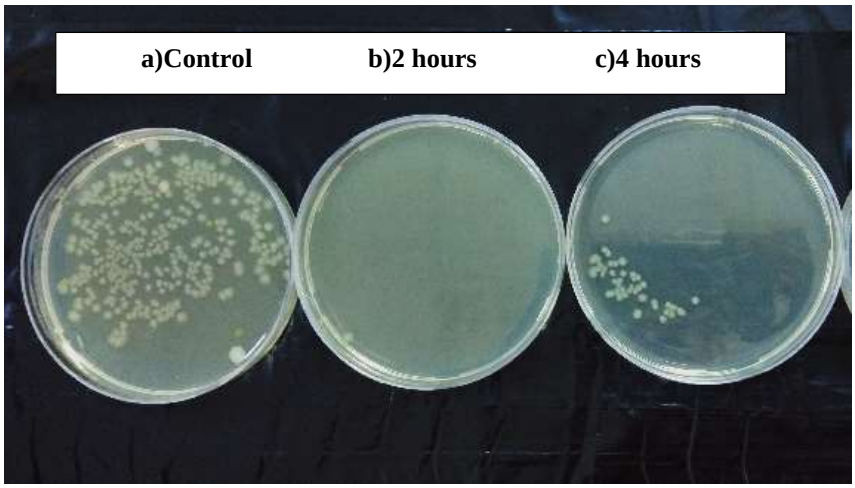

Figure 5. Antimicrobial effects of ZnO-Bent against *E. coli* colonies. *E. coli* cultivated plates incubated ZnO-Bent: a) Control, b) 2 hours of incubation with Zno-Bent, c) 4 hours of incubation with Zno-Bent photocatalyst.

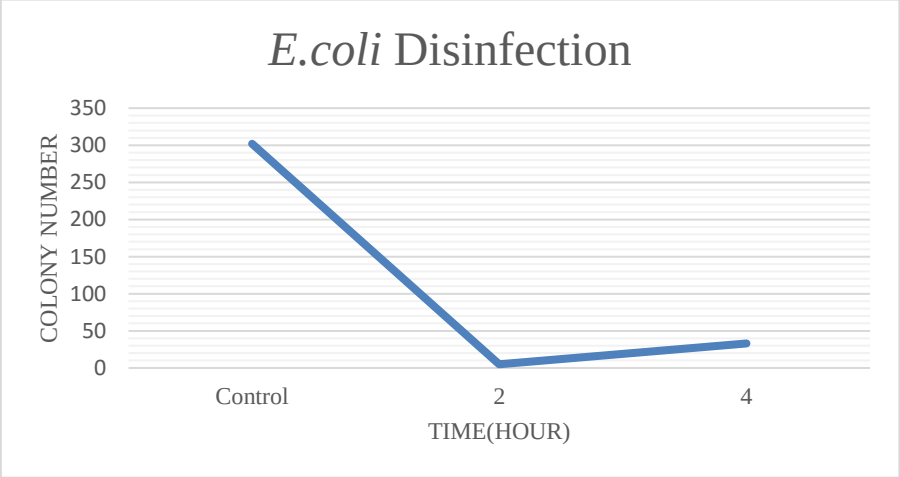

Figure 6. The antimicrobial capacity of ZnO-Bent photocatalys activity under visible light.

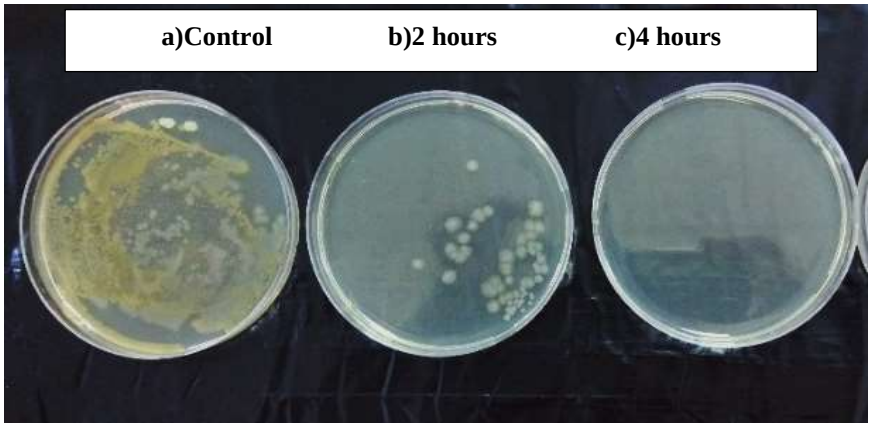

Figure 7. Antimicrobial effects of ZnO-Bent against *P. aeruginosa* Colonies. *P. aeruginosa* cultivated plates incubated ZnO-Bent: a) Control, b) 2 hours of incubation with Zno-Bent, c) 4 hours of incubation with Zno-Bent photocatalyst.

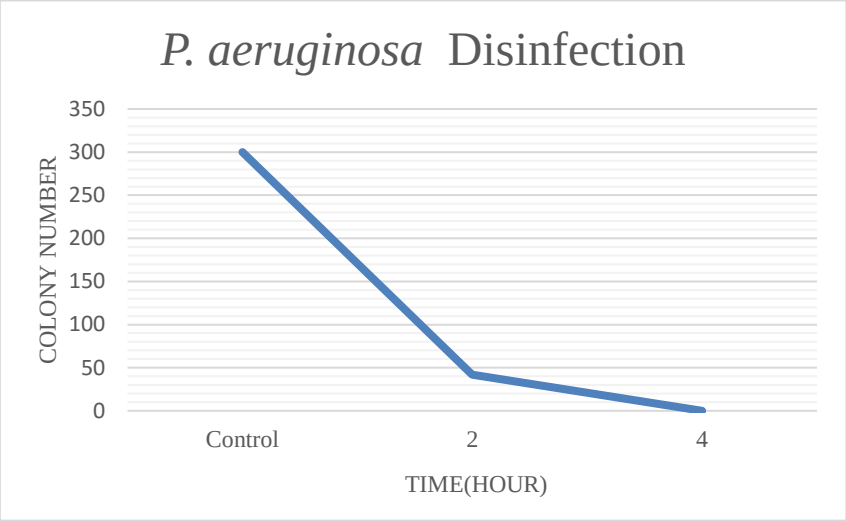

Figure 8. The antimicrobial capacity of ZnO-Bent photocatalyst activity under visible light is presented in a time-dependent manner.

Table 3. Microbicide activities of ZnO-Bent against *E. coli* and *P. aeruginosa* respectively.

	***E. coli* (2 hours incubation)**	***E. coli* (4 hours incubation**	***P. aeruginosa* (2 hours incubation)**	***P. aeruginosa* (4 hours incubation)**
ZnO-Bent	%98.3	%89	%86	%100

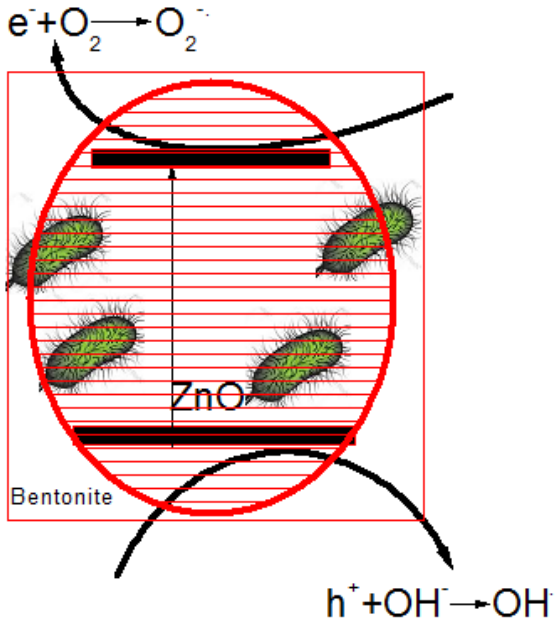

Figure 9. Photocatalytic illustration of disinfection of e-coli under visible light

From Figure 9 when excited the ZnO-Bent catalyst under visible light the valence band electrons transferred to its conductive band level. In this case, the charge carriers which are holes and electrons reacted with H_2O and O_2 to form hydroxide (OH^-) and superoxide ($O_2^{-\cdot}$) radicals respectively [22]. This oxidation process caused to inactivate the *E. coli* and *P. aeruginosa* [23].

4. DISCUSSION

ZnO/Bent photocatalytic inactivation performance against *P. aeruginosa* was highest at the end of 4 hours. ZnO/Bent photocatalytic inactivation performance against *E. coli* was highest at the end of 2 hours. In summary, as synthesized ZnO/Bent particles were spherical morphology with cotton-like bentonite. the ZnO/Bent catalyst was fabricated by introducing the ZnO compound onto the Bentonite surface. The photocatalytic performance of as-synthesized catalysts shows that ZnO/Bent composite exhibits better photoactivity than pure ZnO under visible light. Based on the above results, the enhanced photocatalytic activity for the ZnO/Bent catalyst can be attributed to two major factors. The first one is the efficient inhibition of recombination rate of $^{e^-}/_{h+}$ pairs. This caused more radicals available on the catalyst surface to inactivate the *E. coli* and *P. aeruginosa*. The second one is the higher adsorption ability in the ZnO/Bent system. Photocatalytic mechanism efficiency depends on the particle size of the composite and microorganism type. This research exhibits the efficiency of ZnO/Bent photocatalytic disinfection model against *E. coli* and *P. aeruginosa*. Manuscript expected to offer useful perspectives for the future improvements in this research area.

ACKNOWLEDGMENTS

This study has been supported by Mugla Sıtkı Koçman University Scientific Research Unit with 15/139

CONFLICT OF INTEREST

The authors stated that there are no conflicts of interest regarding the publication of this article.

REFERENCE

[1] Zhang G, Tan Y, Sun Z, Zheng S. Synthesis of BiOCl/TiO_2 heterostructure composites and their enhanced photocatalytic activity. J Environ Chem Eng, 2017; 5: 1196-1204.

[2] Lima AAM, Moore SR, Barboza MS, et al. Persistent Diarrhea Signals a Critical Period of Increased Diarrhea Burdens and Nutritional Shortfalls: A Prospective Cohort Study among Children in Northeastern Brazil. The Journal of Infectious Diseases, 2000; 181(5): 1643-1651.

[3] Singh P, Bengtsson L. Impact of warmer climate on melt and evaporation for the rainfed, snowfed and glacierfed basins in the Himalayan region. Journal of Hydrology, 2005; 300:140-154.

[4] Shannon M, Bohn PW, Elimelech M, Georgiadis JG, Mariñas BJ, Mayes AM, Science and technology for water purification in the coming decades. Nature, 2008; 452: 301-310.

[5] Wang W, Huang G, Jimmy CY, Wong PK. Advances in photocatalytic disinfection of bacteria: development of photocatalysts and mechanisms. Journal of Environmental Sciences, 2015; 34: 232-247.

[6] Gamage J, Zhang Z. Applications of photocatalytic disinfection. International Journal of Photoenergy, 2010; 1-10.

[7] Song L, Pang Y, Zheng Y, et al. Design, preparation and enhanced photocatalytic activity of porous BiOCl/BiVO4 microspheres via a coprecipitation-hydrothermal method. Journal of Alloys and Compounds, 2017; 710, 375-382.

[8] Zhang L, Wang W, Zhou L, Shang M & Sun S, Fe_3O_4 coupled BiOCI: a highly efficient magnetic photocaalyst. Appl Catal B, 2009; 90 (3-4): 458- 462.

[9] Zhang KL, Liu CM, Huang FQ et al. Study of the electronic structure and photocatalytic activity of the BiOCl photocatalyst. Appl. Catal. B Environ, 2006; 68 (3-4): 125–129.

[10] Liu Y, Yao W, Liu D, et al. Enhancement of visible light mineralization ability and photocatalytic of $BipO_4$/BiOI. Appl. Catal. B: Environ 2015; 163: 547-553.

[11] Ma W, Chen L, Zhu Y, et al. Facile synthesis of the magnetic BiOCI/ZnFe2O4heterostructures with enhanced photocatalytic activity under visible light irradiation. Colloids And Surfaces A: Physicochem And Eng. Aspects, 2016; 508: 135-141.

[12] Priya B, Shandilya P, Raizada P, et al. Photocatalytic mineralization and degradation kinetics of ampicillin and oxytetracycline antibiotics using graphene sand composite and chitosan supported BiOCl. J. Mol.Catal. A: Chemical, 2016; 423: 400-413.

[13] Zhang L, Zhang J, Zhang W, et al. Photocatalytic activity of attapulgite-BiOCI-TiO_2 toward degradation of methyl orange under UV and visible light irradiation. Mater Res Bull, 2015; 66: 109-114.

[14] Hartman D, Perfecting Your Spread Plate Technique. J Microbiol Biol Educ. 2011; 12(2): 204-205.

[15] Saelim NO, Magaraphan R, Sreethawong T. Preparation of sol-gel TiO^2/purified Na-bentonite composites and their photovoltaic application for natural dye-sensitized solar cells. Energy Convers Manage, 2011; 52(8–9): 2815–2818.

[16] Sun D, Mao J, Cheng L, Yang X, Li H, Zhang L, Zang W, Zang Q, Li P, Magnetic g-C3N4/NiFe2O4 composite with enhanced activity on photocatalytic disinfection of Aspergillus flavus. Chemical Engineering Journal, 2021; 418: 129417.

[17] Najma B, Kasi AK, Kasi JK, Akbar A, Bokhari SMA, Stroe IR, ZnO/AAO photocatalytic membranes for efficient water disinfection: Synthesis, characterization and antibacterial assay. Applied Surface Science, 2018; 448:104-114.

[18] Karunakaran C, Abiramasundari G, Gomathisankar P, Manikandan G, Anandi V, Preparation and characterization of ZnO–TiO2 nanocomposite for photocatalytic disinfection of bacteria and detoxification of cyanide under visible light. Materials Research Bulletin, 2011; 46(10): 1586-1592.

[19] Cao M, Wang F, Zhu J, et al. Shape-controlled synthesis of flower-like ZnO microstructures and their enhanced photocatalytic properties. Materials Letters, 2017; 192, 1-4.

[20] Soltani, RDC, Jorfi S, Safari M, Rajaei MS, Enhanced sonocatalysis of textile wastewater using bentonite supported ZnO nanoparticles: Response surface methodological approach. Journal of Environmental Management, 2016; 179: 47-57.

[21] Baikousi M, Bourlinos AB, Douvalis A, et al. Synthesis and characterization of γ-Fe2O3/carbon hybrids and their application in the removal of hexavalent chromium ions from aqueous solutions. Langmuir, 2012; 28(8): 3918-3930.

[22] Vaizoğullar Aİ, TiO_2/ZnO Supported on Sepiolite: Preparation, Structural Characterization, and Photocatalytic Degradation of Flumequine Antibiotic in Aqueous Solution. Chem Eng Commun, 2017; 204: 689-697.

[23] Motshekga SC, Ray SS, Onyango MS. Momba MN, Microwave-assisted synthesis, characterization and antibacterial activity of Ag/ZnO nanoparticles supported bentonite clay. Journal of Hazardous Materials, 2013; 262: 439-446.

[24] Paspaltsis I, Kotta K, Lagoudaki R, et al. Titanium dioxide photocatalytic inactivation of prions. Journal of General Virology, 2006; 87(10):3125–3130.

[25] Foster HA, Ditta IB, Varghese S. Photocatalytic disinfection using titanium dioxide: spectrum and mechanism of antimicrobial activity. Applied Microbiology Biotechnology, 2011; 90:1847–1868

[26] Mahon MJ, Pillai SC, Kelly JM, Gill LW. Solar photocatalytic disinfection of E. coli and bacteriophages MS2, ΦX174 and PR772 using TiO_2, ZnO and ruthenium-based complexes in a continuous flow system. Journal of Photochemistry & Photobiology, B: Biology, 2017; 170:79-90.

[27] Oh W-D, Lua S-K, Donga Z, Lim T-T. Rational design of hierarchically structured CuBi2O4 composites by deliberate manipulation of the nucleation and growth kinetics of CuBi2O4 for environmental applications. Nanoscale 2016; 8:2046-2054.

ESKİŞEHİR TEKNİK ÜNİVERSİTESİ BİLİM VE TEKNOLOJİ DERGİSİ C- YAŞAM BİLİMLERİ VE BİYOTEKNOLOJİ

Eskişehir Technical University Journal of Science and Technology C- Life Sciences and Biotechnology

2022, 11(1), pp. 22-30, DOI: 10.18038/aubtdc.1051707

RESEARCH ARTICLE

SIMULTANEOUS QUANTITATIVE ANALYSIS OF TWO ANTHELMINTIC DRUGS IN A VETERINARY DOSAGE FORM

Eda BÜKER[1,*], Nagihan YAŞAR [2], Erdal DİNÇ [2]

[1] Department of Basic Pharmaceutical Science, Faculty of Pharmacy, Gazi University, Ankara, Turkey
[2] Department of Analytical Chemistry, Faculty of Pharmacy, Ankara University, Ankara, Turkey

ABSTRACT

In this research article, a new chromatographic method ultra-performance liquid chromatography (UPLC) method was developed for the quantification of ivermectin (IMT)-preziquantel (PRZQ) in a two-component mixture and veterinary dosage form mixture. The separation of the studied veterinary drugs (IMT and PRZQ) was carried out on Waters Acquity ® BEH C18 column (50mm x 2.1 mm i.d., 1.7 m) using a mobile phase consisting of water-acetonitrile-methanol (10:70:20, v/v). In the chromatographic analysis, flow rate was 0.38 mL/min, and column temperature was maintained at 42 0C. The chromatographic detection of IMT and PRZQ was made at the wavelength of 220.0 and 245.0 nm, respectively. The developed UPLC method was validated and applied to real samples consisting of IMT and PRZQ. Recovery assay results were found to be 100.4 % for PRZQ and 101.8 % for IMT. The presented UPLC method is introduced as an alternative choice for the quality control of pharmaceutical preparations containing these drugs. For the quality control of pharmaceutical preparations containing these drugs, the presented UPLC method is introduced as an alternative experimental analysis choice.

Keywords: Ultra performance liquid chromatography, Ivermectin, praziquantel, Anthelmintic veterinary dosage form

1. INTRODUCTION

Parasites cause failure to show normal performance and productivity in animals, sensitivity to diseases in animals, weakening as a result of insufficient use of food, enlargement of postpartum spaces, deterioration of hair cover, diarrhea, and death in more severe cases. Anthelmintic drugs are used to treat parasites in animals. These drugs include ivermectin (IMT) and praziquantel (PRZQ).

Ivermectin, one of the drugs that disrupt neuromuscular coordination, is effective in parasites by mimicking neurotransmitters or changing their effects. Eventually, the parasite becomes paralyzed. Spastic or loose paralysis in parasites causes them to be expelled by normal peristaltic movements of the intestines [1]. Praziquantel, an isoquinoline compound, is effective in neurotransmission. The parasite increases cell membrane tension, causing depolarization and contraction. It facilitates the passage of glucose through the parasite skin [2, 3].

A literature survey showed that the simultaneously quantification of ivermectin and preziquantel in their binary mixture and their combinations with other active substances was reported, including ultraviolet spectroscopy [4], diffuse reflectance spectroscopy [4] high-performance liquid chromatography [5-9], high-performance thin layer chromatography [10] and high-performance liquid chromatography with tandem mass spectrometry [11].

In the comparison of the methods, the newly developed UPLC method has shorter retention time than that of traditional HPLC method in [12].

*Corresponding Author: edabiyik@gazi.edu.tr; eda_buker@yahoo.com
Received: 10.09.2021 Published: 19.01.2022

UPLC or HPLC method is useful technique for the separation and analysis of analytes in complex mixtures. In previous studies, it was observed that the traditional HPLC was used to the simultaneous quantitative analysis of the related veterinary drugs. However, the literature method has time consuming with long runtime and the studies for the analysis of analytes. Therefore, the improved of new UPLC method is a reasonable to get short runtime with low cost. In this study, a new UPLC method with Photodiode Array (PDA) detection was developed for the quantitative resolution of a two component mixture or a combined veterinary dosage forms containing the studied veterinary active compounds. The validity of the developed UPLC approach was performed by analyzing validation samples, synthetic mixtures, intra-day and inter-day samples, and standard addition samples. IMT and PRZQ in the veterinary tablets were determined by using the newly improved UPLC method.

2. MATERIAL AND METHODS

2.1. Standard, Chemical and Samples

Standards of ivermectin (99.6 %), and praziquantel (99.7 %) were get from Sigma-Aldrich. Acetonitrile and methanol (UPLC grade) were obtained from Merck. Ultrapure water was acquired using a Milli-Q purification system from Millipore (Milford, MA, USA). The commercial formulation, Dicromec tablet consisting of PRZQ and IMT was obtained from a pharmacy, Ankara, Turkey.

2.2. Preparation of Solutions

Stock solution of 10 mg/100 mL of IMT and PRZQ were individually prepared in methanol. A series of the calibration solutions consisting of 16 solutions at 8 different concentrations in the range of 2.0-44.0 µg/mL for IMT and 20.0-160.0 µg/mL for PRZQ was prepared by using the stock solutions.

Validation test set containing 17 different concentrations compounds in the working range of 2.0-44.0 µg/mL for IMT and 20.0-160.0 µg/mL for PRZQ was prepared.

Standard addition samples consisting of an appropriate amount of veterinary formulation at a constant concentration; IMT and PRZQ at four different concentration levels 5.0 µg/mL, 10.0µg/mL, 20.0 µg/mL, and 30.0 µg/mL for IMT and 10.0 µg/mL, 20.0 µg/mL, 30.0 µg/mL, and 40.0 µg/mL for PRZQ were prepared. Three different concentrations of IMT containing IMT and PRZQ in the working ranges between 2.0-44.0 µg/mL for IMT (at three different concentration levels 2.0 µg/mL, 26.0 µg/mL and 44.0 for µg/mL) and 10.0-80.0 µg/mL for PRZQ (at three different concentration levels 10.0 µg/mL, 60.0 µg/mL and 80.0 µg/mL) intra-day and inter-day solutions were prepared, respectively.

2.3. Preparation of Veterinary Tablet Sample

10 tablets, each containing 10.0 mg IMT and 250.0 mg PRZQ, was weighted and finely powdered in a mortar. An amount of this powder equivalent to the average mass of half tablet of DICROMEC® (Anatolia Medicine & Chemical Industry Co., Konya,Turkey) was weighted, dissolved in the solvent mixture by sonication, than diluted to 50 mL. The stock mixture prepared in the balloon was mixed with a magnetic stirrer for 35 minutes and filtered through a membrane filter (Sartorius Minisart = 0.20 µm). After 4 mL of this stock solution was taken and added into a 10 mL flask, the volume was made up the mark with methanol.

The solution was filtered by a syringe filter (Acrodisc, Pall Industries). This procedure was repeated 10 times.

2.4. Experimental Conditions of UPLC

Waters Acquity Series UPLC System (Waters Corporation 34 Maple Street Milford, MA 01757 USA) (with PDA system) was used for the chromatographic quantification of PRQ and IMT. The system was operated up by Empower UPLC Software program.
The analytical separation was achieved on an Waters Acquity ® BEH C18 column (50mm x 2.1 mm i.d., 1.7 m) maintained at 42 0C. The mobile phase consisted of water-acetonitrile-methanol (10:70:20, v/v). The isocratic flow rate was 0.38 mL/min and the injection volume was 1 µL. The needle was washed with 2 µL of acetonitrile/methanol (50:50 v/v) between injections.

3. RESULTS AND DISCUSSION

Many mobile phase systems containing various organic solvents, such as water, methanol and acetonitrile, at different amount of solvents were tried to find the optimum conditions to get desirable elution of IMT and PRZQ. By using the Waters Acquity ® BEH C18 column (50mm x 2.1 mm i.d., 1.7 m), a mobile phase consisting of water-acetonitrile-methanol (10:70:20, v/v), with isocratic flow rate of 0.38 mL/min and column temperature of 42 0C, was found appropriate for adequate elution of IMT and PRZQ in samples. The injection volume for the sample was 1 µL for the chromatographic procedure. As stated in Figure 1 A and B, the optimum chromatographic detection for IMT and PRZQ was carried out at 220.0 nm and 245.0 nm, respectively. The concentration set consisting of IMT and PRZQ in the working ranges between of 2.0-44.0 µg/mL and 20.0-160.0 mg/mL were gotten by using the stock solutions of the related drugs. The UPLC chromatograms for the calibration samples of IMT and PRZQ were registrated according to optimized chromatographic conditions, as shown in Figure 1 A and B, respectively). A analogue chromatographic treatment was used to the standard addition samples and commercial veterinary samples. From Figures 1 A and B, the retention time of IMT and PRZQ were found as 0.482 minutes, 0.720 minutes, respectively. Calibration curves for IMT and PRZQ were calculated using linear regression analysis between concentration and peak-area ratio 220.0 nm and 245.0 nm, respectively. The statistical results for the calculations were listed in Table 1. IMT and PRZQ in the veterinary tablets were determined via the calibration curves.

Table 1. Results of linear regression analysis

	PRZQ	IMT
m	5744	6023.5
n	18448.4	288.6
r	0.9992	0.9997
SD(m)	95.4	58.8
SD(n)	482	157.6
SD(r)	6185.8	2287.1
LOD	2.52	0.78
LOQ	8.39	2.62

m = The slope of the linear regression equation
n = The cutoff point of the linear regression equation
r = Correlation coefficient of linear regression equation
SD (m) = Standard deviation of slope
SD (n) = Standard deviation of the cutoff point
SD(r) = Standard deviation of the correlation coefficient
LOD = Limit of detection (µg/mL)
LOQ = Limit of quantification (µg/mL)

The UPLC peak results of the concentration sample set involving of were depicted in Figure 1 A and B. From these UPLC chromatograms, the elution times of IMT and PRZQ were observed as 0.482 min and 0.720 min, respectively.

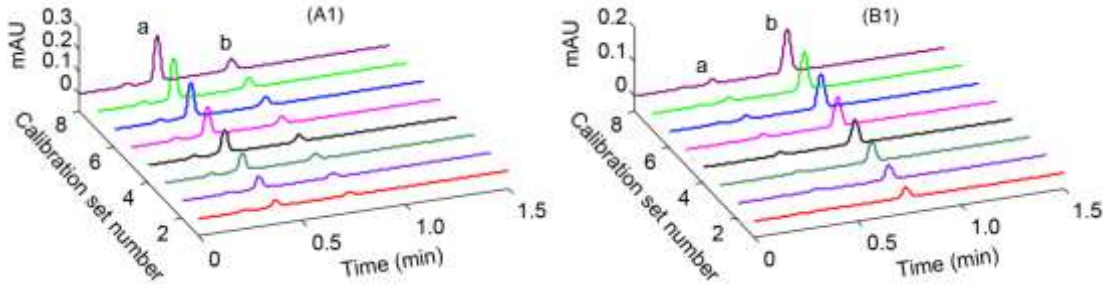

Figure 1. Chromatograms of calibration set were obtained by applying the chromatographic condition to the calibration samples (CS number) for separated compounds IMT (A1, 220.0 nm (a) and PRZQ (B1, 245.0 nm) (b).

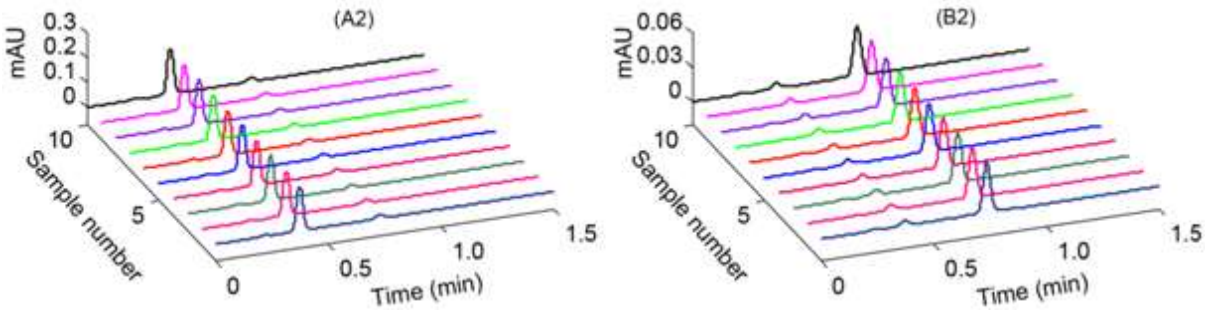

Figure 2. Chromatograms of Dicromec commercial veterinary samples A2 (220 nm) and B2 (245 nm) for IMT and PRZQ active compounds, respectively.

This study showed that the proposed and validated UPLC technique gave us a good separation of the analytes with short analysis time of 1.5 min. The results showed that, the newly improved UPLC technique was very promising to accomplish the rapid and dependable analysis of the veterinary tablet preparation containing IMT and PRZQ.

3.1. UPLC Method Validation

As explained in the section Standard solutions, a concentration set of the mixture solutions consisting of IMT and PRZQ was prepared then, under optimal chromatographic conditions, the UPLC results of the concentration set were plotted by PDA detection at the wavelength, 245.0 nm for IMT and 220.0 nm for PRZQ. Calibration graphs for IMT and PRZQ with high correlation coefficients were obtained. Their statistical data consisting of concentration ranges, slope, intercept and correlation coefficients of the linear regression equations, limit of detection (LOD) and limit of quantification (LOQ) were presented in Table 1. For both IMT and PRZQ, suitable linearity's having advanced correlation coefficients were detected (see Table 2.). The LOD and LOQ values of IMT and PRZQ were given in Table 1.

An objective set consisting of 17 different mixture samples of IMT and PRZQ in the different mixture compositions was analyzed by the newly developed UPLC method. Recovery results and relative standard deviations were calculated and shown in Table 2. As it was seen in from Table 2, recovery

values were 101.6% for IMT and 99.7% for PRZQ, and relative standard deviation values were 1.87% for IMT and 1.36% for PRZQ. It was deduced that the newly improved UPLC technique has a good accuracy and precision for the UPLC analysis of IMT and PRZQ.

Table 2. Analysis results were obtained from the optimized and validated UPLC method of IMT and PRZQ synthetic mixture solutions.

Added (µg/µL)		Found (µg/µL)		Recovery (%)		
Mix no.	PRZQ	IMT	PRZQ	IMT	PRZQ	IMT
1	10	3	9.8	2.9	97.6	95.4
2	20	3	20.4	3.0	101.8	101.4
3	30	3	29.8	3.1	99.4	102.0
4	40	3	40.1	3.0	100.4	101.1
5	50	3	49.4	3.1	98.8	103.3
6	60	3	61.4	3.1	102.3	102.6
7	70	3	70.5	3.1	100.8	101.9
8	80	3	81.0	3.0	101.3	101.6
9	75	2	74.8	2.0	99.8	102.4
10	75	8	75.2	8.2	100.2	102.1
11	75	14	74.2	14.3	99.0	101.9
12	75	20	73.6	21.0	98.2	104.9
13	75	26	74.0	26.4	98.7	101.4
14	75	32	74.5	32.4	99.4	101.2
15	75	38	75.4	38.2	100.5	100.6
16	75	44	73.6	44.8	98.1	101.8
17	75	3	73.9	3.0	98.6	101.5
				Mean	99.7	101.6
				SD	1.36	1.87
				RSD	1.36	1.84

SD = Standart deviation
RSD = Relative standard deviation

Selectivity/ specificity for the UPLC technique was checked according to presence or absence of the excipient's effect on the analysis of IMT and PRZQ from veterinary tablet dosage form. As explained in the section 2.2, the standard solutions were prepared by adding of the stock solutions of IMT (at four different amounts; 5.0, 10.0, 20.0, and 30.0 µg/mL) and PRZQ (at four different amounts; 10.0, 20.0, 30.0, and 40.0 µg/mL) to the sample solution of veterinary tablet dosage form. From the Table 4, it was observed that there is no interference of the veterinary tablet's excipient on the determination of analytes.

Accuracy and precision testing for the newly improved UPLC method were performed with the analysis of the intra-day and inter-day samples. The samples containing IMT (at three different concentrations: 2.0, 26.0, and 44.0 µg/mL) and PRZQ (at three different concentrations: 10.0, 60.0, and 80.0 µg/mL) were analyzed. Intra-day and inter-day experiments were carried out at different three times and at different three days with three replications, respectively. Experiment for each concentration level was repeated three times. Mean recoveries; relative standard deviations and relative standard errors were calculated and shown in Table 3. These analyses indicated that the newly improved UPLC method is suitable to analyze the related compounds in samples with required precision and accuracy.

Table 3. Analysis results of intra-day and inter-day samples

	Added (µg/µL)		Found (µg/µL)	
	PRQ	IMT	PRZQ	IMT
Inter-day	10	2	10.39	2.03
	60	26	60.48	26.68
	80	44	82.98	46.13
Intra-day	10	2	9.93	2.00
	60	26	60.21	26.15
	80	44	81.14	46.09
			Recovery (%)	
			PRZQ	IMT
Inter-day			103.9	101.6
			100.8	102.6
			103.7	104.8
Intra-day			99.3	100.0
			100.4	100.6
			101.4	104.8
			RSD (%)	
			PRZQ	IMT
Inter-day			0.82	2.61
			0.49	1.19
			0.22	0.16
Intra-day			1.05	4.36
			0.98	0.67
			1.08	1.58
			RSE (%)	
			PRZQ	IMT
Inter-day			3.85	1.58
			0.80	2.61
			3.72	4.84
Intra-day			-0.65	0.00
			0.35	0.56
			1.43	4.76

RSD = Relative standard deviation
RSE = Relative standard error
n= 3 (for all concentration level)

Table 4. Analysis results of standard addition sapmles

	Added		Found (µg/mL)	
	PRZQ	IMT	PRZQ	IMT
Formulation	10	5	9.69	5.06
Formulation	20	10	19.62	9.98
Formulation	30	20	29.20	20.20
Formulation	40	30	40.40	30.65
			Recovery (%)	
			PRZQ	IMT
			96.9	101.3
			98.1	99.8
			97.3	101.0
			101.0	102.2
			RSD (%)	
			PRZQ	IMT
			0.47	0.10
			0.46	0.43
			0.47	0.54
			1.09	0.69

RSD = Relative standard deviation

3.2 UPLC Method Application to Veterinary Tablet

After the method validation step, the newly developed UPLC technique was employed to simultaneously quantify IMT and PRZQ in commercial veterinary formulation. The UPLC chromatograms of these industrial veterinary samples were plotted under separation conditions. The peak areas of IMT and PRZQ obtained at the retention times, 0.482 min and 0.720 min were computed and replaced into the calculations of the calibration curves to determine the related drugs in veterinary tablet dosage form, respectively (see Figure 2.). Assay results obtained from veterinary tablet dosage form samples were shown in Table 5. As it was seen in the experimental results listed in Table 5, the improved UPLC technique is very appropriate for the quantitative analysis of IMT and PRZQ in the studied veterinary tablet dosage form.

Table 5. Quantitative analysis results of IMT and PRZQ in commercial veterinary preparation (Label claim: PRQ 250.0 mg/mL and IMT 10.0 mg/mL).

Exp no.	PRZQ µg/µL	IMT µg/µL
1	245.43	9.87
2	246.10	10.02
3	246.91	9.59
4	246.93	9.70
5	248.98	9.38
6	242.94	9.56
7	244.58	9.70
8	240.77	9.64
9	246.24	10.23
10	255.27	9.76
Mean	246.4	9.7
SD	3.86	0.24
RSD	1.57	2.50

SD = Standard deviation
RSD =Relative standard deviation

4. CONCLUSION

In our work, a new UPLC technique was improved for the simultaneous analysis of the substance of IMT and PRZQ in industrial veterinary tablet preparation with short runtime and few experiments. In the development of selective, precise, accurate and reliable UPLC technique a equilibrium between high-quality separation and short analysis time was considered. Thus, the analysis by the improved UPLC method were accomplished within a short runtime of 1.5 min with a good separation of the IMT and PRZQ peaks in a UPLC chromatogram. In evaluated with HPLC (12), the newly applied UPLC is more economical with suitable chromatographic separation of IMT and PRZQ in an industrial tablet formulation. It was concluded that the proposed UPLC method was a very useful and promising for the simultaneous quantification and routine analysis of the active compounds, IMT and PRZQ in commercial veterinary tablets.

CONFLICT OF INTEREST

The authors stated that there are no conflicts of interest regarding the publication of this article.

REFERENCES

[1] Del Guidice P, Marty P. Ivermectin: A new therapeutic weapon in dermatology? Arch Dermatol, 1999;135:705-6.

[2] Takayangui OM. Neurocisticercose avaliacao da terapeutica com praziquantel. [Neurocysticercosis. II. Evaluation of treatment with praziquantel. Arq Neuro-Psiquiat, 1990; 48(1): 11–15.

[3] Koul PA, Waheed A, Hayat M, Sofi BA. Praziquantel in niclosamide-resistant Taenia saginata infection. Scand J Infect Dis, 1999; 31(6): 603–4.

[4] Piantavini MS, Pontes FL, Weiss LX, Senab MM, Pontarolo R. Comparison between ultraviolet and infrared spectroscopies for the simultaneous multivariate determination of pyrantel and praziquantel. J Braz Chem Soc, 2015;26(7):1387-95. doi:10.5935/0103-5053.20150107

[5] Phatak HM, Vaidya VV, Phatak MS, Rajeghadge D. A rapid high performance liquid chromatography method for simultaneous quantification of praziquantel, ivermectin and abamectin from veterinary formulations: Development, validation and application. Int J Pharm Res Scholars, 2016;5(1):57-65.

[6] Vijay Kumar G, Sravanthi B, Praveen A. Analytical method development and validation for ivermectin and albendazole in combine dosage form by RPHPLC. Int J Curr Trends Pharma Res, 2019;7(1):7-12.

[7] Bhavya B, Nagaraju P, Mounika V, Priyadarshini GI. Stability indicating RP-HPLC method development and validation for simultaneous estimation of albendazole and ivermectin in pharmaceutical dosage form. Asian J Pharm Anal, 2017;7(1):6-14. doi:10.5958/2231-5675.2017.00002.3

[8] Rupali S, Shyamala B, Kulesh K, Shailendra KJ. Simultaneous estimation of pyrantel pamoate, praziquantel & febantel by high performance liquid chromatography using dual wavelength. J Appl Pharm Res, 2014;2(2):32-43.

[9] Rajesh R, Jithu JJ. A validated RP-HPLC method for simultaneous estimation of pyrantel pamoate and praziquantel in bulk and pharmaceutical dosage form. Int J Pharm Pharm Sci, 2019;11(5):62-7. doi:10.22159/ijpps.2019v11i5.30488

[10] Kumudini SR, Sunil RD, Vidhya KB, Amruta LS. Validated HPTLC method for simultaneous estimation of ivermectin and albendazole in formulation. Asian J Pharm Biol Res, 2011;1(3):330-6.

[11] Pontes FL, Pontarolo RO, Campos FR, Gasparetto JC, Cardoso MA, Piantavini MS, et al. Development and validation of an HPLC-MS/MS method for simultan ous determination of ivermectin, febantel, praziquantel, pyrantel pamoate and related compounds in fixed dose combination for veterinary use. Asian J Pharm Clin Res, 2013;6(2):191-9.

[12] Gandla K, Lalitha R, Varun D, Shruthi P, TejaVR Analytical Method Validation of Ivermectin and Praziquantel in Bulk and Pharmaceutical Dosage Form by UPLC, International Journal of Research Publication and Reviews, 2021; 2 (4):573-583.

ESKİŞEHİR TEKNİK ÜNİVERSİTESİ BİLİM VE TEKNOLOJİ DERGİSİ C- YAŞAM BİLİMLERİ VE BİYOTEKNOLOJİ

Eskişehir Technical University Journal of Science and Technology C- Life Sciences and Biotechnology

2022, 11(1), pp. 31-38, DOI: 10.18038/aubtdc.907029

REVIEW

WHAT TELL US THE BIONUMBERS FOR PROTEIN PHOSPHORYLATION IN PLANT DEFENSES

Berna BAŞ*

ABSTRACT

Plants to survive against to devastating impact of invasive biotic agents have to powerfully struggle in armed combat with microorganisms. Therefore they need to activate rapidly and efficiently pre-existing potential defensive chemicals. As soon as perception initial external stimuli through plant cell membrane receptors and/or cytoplasmic resistance proteins before activity of related genes, some proteins participated in plant immunity undergo alterations referred as molecular modification. Phosphorylation is one of the first steps and most important modifications in signal transduction pathways of plant immunty. While transcription/translation of the gene dependening to molecular size, organism type, ribosome number is proceed in time unit from seconds to minutes, whereas phosphorylation is occurred in the time period expressed with milliseconds/seconds. Why does protein phosphorylation in plant cells occur quickly in comparison to gene expression? In this commentary work inquired of this question, speedity of gene expression and phosphorylation processes on time profile is compared outlining with bionumbers.

Keywords: Bionumbers, Protein/amino acid phosphorylation, Time-course of phosphorylation, Plant defense

1. INTRODUCTION

Due to be continuously exposed to external stimuli in sub-optimal surroundings, plants have to speedly respond to biotic and abiotic agents. Unlike vertebrates, intermediary molecules in plant immune system do not circuit throughout plant in motion. If the subversive actions started at the point of infection by the invader cannot be defeated with versatile plant defense strategies for pathogen defense, defense genes with long-distance are prompted at whole plant level. Biotic elicitor-effector molecules as non-self or self-modified stimulus in plants are recognized by plant cell surface sensors or cytoplasmic receptors. Initial alterations upon biotic stress sensing in plants, rather genetic regulation, are molecular modifications of the molecules participated to plant immune system such as the change of self-defense molecules or receptor proteins. Molecular modifications include chemical, physical and biological construct alterations in molecules [1]. Thus, this is caused generation of new variations derived from compounds undergoing change. In medicine, molecular modification is most widely used term for chemical changing of any molecule to design drugs [2]. Also chemical modificationis the changing with reagents of structure of biological macromolecules like proteins, nucleic acids, polysaccharides (UIPAC, 1997: The International Union of Pure and Applied Chemistry, Compendium of Chemical Terminology). However, post-translational modifications (PTMs) are related to the chemical modification process of proteins with addition into or removal from target molecule of functional group, any ion, small molecules after protein biosynthesis occured, it may be considered within chemical modification. Till now more than 90,000 individual PTMs were explored [3]. Eventually these chemical reactions without altering basic scaffold of molecules vary physical structure of molecule, consequently their biological functions change as well. In plant immunity, the term "chemical modification" is not originally used in its genuine content in actually. But it is attempted to draw manipulations by chemical process ascribed to resembling to chemical modification. Plants have a wide group of chemical modifications involvement in phosphorylation, acetylation, methylation, sumoylation, proteolysis, glycosylation chemical reactions, named as PTMs

*Corresponding Author:bbas65@hotmail.com
Received:31.01.2021 Published: 19.01.2022

[4,5]. PTMs are vitally significant to modulate functions of proteins that play role in cell metabolism, in operating of intracellular signal transduction pathways, in promoting cell differentiations, division and proliferation [6,7,8,9]. Amongst PTM varieties, phosphorylation is the most studied and the best known sort of chemical modification [5,10]. Moreover, it has also the most data with proteome-wide input [11].

Since database records of phosphorylation of key molecules responsible for almost all biological regulations are registered in many various scholarly websites, they are always updated with new phosphoproteomic data input (**http**://www.p3db.org/;**http**://phosphat.mpimp-golm.mpg.de/;**http**://www.cbs.dtu.dk/services/NetPhos/; **http**://iekpd.biocuckoo.org/). For instance, by now there are records of 197348 phosphorylation regulators, 109912 protein kinases, 23294 phosphatases, 68748 phosphoprotein binding domains belonging to 164 eukaryotic species. Moreover 47 of these are in plants (http://iekpd.biocuckoo.org website). However, the reports of large-scale comparative analysis and time-course of phosphorylation corresponding plant immunity are restricted with a few model plant species. For works directly on quantity of time-course of phosphorylation about plant defense proteins, it should be solely referred to Schulze et al [12].

While protein/amino acid phosphorylation reaction which allows shifting of protein activities rapidly in a very short time [13] is occured within seconds/milliseconds, synthesizing of a new protein is taken place within minutes. Why do some cells first react to a biotic/abiotic signal by phosphorylation? In this short commentary evaluated from different perspective of this issue, time intervals of phosphorylation reaction with gene expression have been compared using bionumbers.

2. TYPES OF PTMs

Plants exposed to harsh ambient conditions have to reply rapidly and efficiently to cope with external detrimental stimuli come from biotic/abiotic variables. Althouh more than 200 different types of PTMs have been determined [14], some of the most common PTMs can be functionally classified into subgroups as shown Figure 1. Chemical modifications of proteins related to manage direction of signaling systems and metabolic changing is mainly reversible, but modifications through alterations in structure of polypeptide backbone such as deamidation, eliminylation or amino acid substitution are irreversible [5, 15]. PTMs cause to shift on enzyme activities, inter/intra-molecular conformational changes in proteins, replacement of subcellular location of proteins and variations in protein-protein and protein-other molecule interactions.

Reversible phosphorylation plays much significant role for perceiving of environmental stresses, for transduction of signals throughout membrane in the cell, to multiple intracellular signals, to express immune response, to regulate cell-cycle control mechanisms and to sense endogenous hormones [16, 17, 18]. Conventionally in chemistry, phosphorylation of a molecule is chemically addition of terminal phosphoryl (PO_3^-) group of ATP as phosphate source to an organic molecule. Also removal of phosphorus from any substrate is dephosphorylation. In addition either activities of phosphorylation reaction are catalyzed diverse kinases and phosphatases, respectively. Protein phosphorylation is occurred on most commonly specific amino acid side chains in proteins. Protein kinase enzymes facilitate to be carried phosphate groups of ATP to serine or threonine or tyrosine residue in proteins [19, 20, 21]. Proteins/amino acids/enzymes phosphorylation entailed to alterations of structural conformations of molecules allows to emerge derivative new molecule forms [22] in shortest possible time. For instance, when membrane receptor proteins are phosphorylated with inter/intra molecular interactions upon directly/indirectly attached to microbial elicitors/effectors molecules is subjected to conformational change, a plant perceives this molecular transformation as disruption of normal homeostasis. Consequently the novel derivative molecules gain the competence to stimulate specific events series deployed in plant defense system.

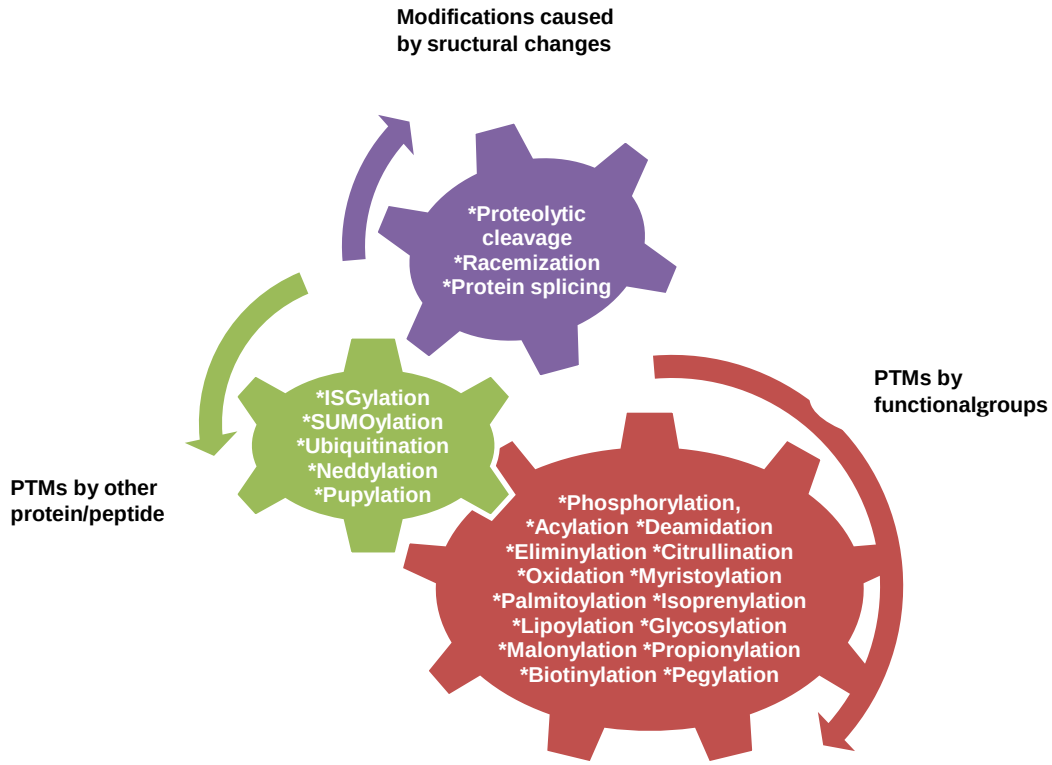

Figure 1. Post-translational modification types [3,14].

It is estimated that there exist hundreds of protein kinases and phosphatases in plants and animals [23]. While Benschop et al. [24] has determined about 1170 phosphopeptide sites on 472 phosphoproteins in Arabidopsis cell culture, Al-Momani et al. [25] has reported ~6500 phosphopeptides identified from over 3000 phosphoproteins in *Arabidopsis*. Li et al. [18] identified 1522 unique peptides, of which 1365 were phosphorylated in rice seedlings, some after infections and some associated with biological processes. Weintz et al. [26] has characterized almost close to 7000 phosphorylation sites on 1800 phosphoproteins against to lipopolysaccharide activation in animals. In actually, these bionumbers show importance and complexity of sophisticated phosphorylation network and the size of the cumulative area occupied by phosphorylation in the eukaryotic genome.

3. PHOSPHORYLATION REACTIONS DEVELOP WITHIN SECONDS

Schulze et al. [12] quantified phosphorylation rate with experimental studies in the time-course analyses of phosphorylation with *Arabidopsis thaliana* FLS2-BAK1 complex protein. Bacterial elicitor Flg22 is perceived by FLS2-BAK1 complex which is an *Arabidopsis* cell membrane receptor. *De novo* phosphorylation trials indicated which measurable phosphorylation has been detected in the 15^{th} second after treatment with flg22 of *Arabidopsis* cells. Furthermore, the reaction has been occurred just before plant immune response is aroused [12]. Also Haj Ahmed et al. [27] published results of the analysis of phosphorylation time-course works such as rapid phoshorylations of NADPH-oxidases and Ca^{+2}-ATPase enzymes, dephosphorylations of H^{+}-ATPases initiated by triggering of up-regulation of plant cell surface receptors. They applied to tomato cell culture a peptide hormone systemin as stimulant to mediate for induction of signal transduction defense pathways in injured plants by herbivory insect damage. Systemin susceptibility reaction has been quantifed from phosphorylation time-course evaluations. After systemin treatment, they assessed situations of phosphorylation, dephosphorylation, not responsive phosphopeptide from a total of 3312

phosphopeptide patterns. Accordingly, in time profile of phosphorylation on their notification, protein enhancement was not observed in the period expressed in minutes. However, incremental phosphopeptide amount (both phosphorylation and dephosphorylation) was explained as change of phosphorylation status. Likewise in an assay directed by phytochrome-mediated photoresponses using foliage protein from *Avena sativa* seedlings, it was revealed that half-time of protein phosphorylation/dephosphorylation reactions reached approximately in 2 seconds at 0℃ under their laboratory conditions [28].Whereas *in vitro* radioactive labelled phosphorus from ATP was transferred into endogenous protein kinases as intermediate from plasma membrane fractions of corn root cells in less than 30 seconds [29].

Similarly, Briskin [30] indicated quantification of enzyme phosphorylation/dephosphorylation reaction kinetic parameters by time-course ratios in red beet plasma membrane H-ATPase enzyme during *in vitro* under different conditions. According to their outcomes, in presence of $MgSO_4$ and radioactive labelled substrate (P) mixture at pH 6.5 at 10℃ phosphoenzyme formation rate $k = 3.24\ s^{-1}$ was reported, and also to the enzyme saturation with its substrate was attained in 600 milliseconds. After 20 seconds pre-incubation of enzyme-radioactive labelled substrate subsequently addition of $MgSO_4$, phosphoenzyme formation rate, $k = 7.46\ s^{-1}$ was calculated. Although existence of magnesium reduced the binding speedity of phosphorus to enzyme, both of two cases [γ-32P]-ATP phosphorus group was carried to the enzyme within milliseconds.

One of the earliest works in this field was published in 1976 [31]. According to Rose and Dube [31]'s results, phosphorus incorporation from phosphoenzyme into phosphoglycerate took places in 38 seconds at 4℃. But this kinetic parameter was too fast to measure at 25℃ and finally reaction was completed in as little as 22 milliseconds. Although phosphorylation reaction is strikingly occurred quickly within milliseconds, it should be regarded this result was obtained from *in vitro* laboratory conditions. Also this data might be possibly variable in living plant cells when environmental factors are changed, nevertheless it should not be expected unusual time variation as more as minutes or hours for the time intervals of phosphorus transference.

The rate of a protein synthesis or transcription process in eukaryotic organisms in comparison with length of time of phosphorylation duration from reports explained above is rather slow. The studies particularly relevant with the time course of phosphorylation of the plant immune molecules is fairly former and a few and also insufficient for the specific issue addressed herein. Tang et al. [32], Park et al. [33], Minkoffet al. [34], Yin et al. [35] have reported qualitative results that phosphorylation of plant immune molecules (proteins) is rapidly occurred without defined exact time intervals. This may be due to the fact that protein phosphorylation is a fast and transient dynamic period and makes difficult to quick measurement of phosphorylation ratio in small area occupied by phosphorus with currently application techniques. Besides the concentration of signal molecules in cell is at low level and experimental models/strategies with range of analytic measurement techniques in use has the limitated capacity, so the stoichiometry of phosphorylation of protein/amino acids is at low level [36]. Nevertheless this preliminary informative inferences display that plants may readily adapt with quick phosphorylation responses to biological systems which are rearranged by environmental suppressions against disturbance caused by external biotic factors in the plant cells for evolution of the long range plant defense signaling.

4. THE RATE OF TRANSCRIPTION AND TRANSLATION

The rate of transcription and translation alters depending on the identification techniques, the cell and organism types, and ribosome number. Studies on the kinetics of gene expression in mammal cells show that the rate of transcription is 1000 nucleotide/minute, this means it is generated 1 kb/minute mRNA [37]. According to Lewin [38], protein synthesis ratio (translation rate) is 140 amino acids/minute, the synthesis of protein molecule in the chain length about of 1000 amino acids residue

drives almost 10 minutes. According to Rawn [39] and Alberts et al. [40], while RNA elongation in mammals and bacteria are 30 nucleotide/second and 30-85 nucleotid/second, respectively, protein synthesis also is 10 amino acid sequences in a second and 50 nucleotide/second = 18 amino acid/second.

Transcription and translation in mammals may take minutes depending on the protein property. When the ratio measurements of phosphorus transfer by Rose and Dube [31] were simply calculated according to results of Hargrove et al [37], the translation of the phosphoenzyme is expected to complete in 131.5 seconds. Based on results of Hargrove et al [37] it might be considered molecular weight of each subunit as approximately ~29.000 da in size containing of ~263 amino acid residues (*****). However by Rawn [39] and Alberts et al. [40], the generation of the same phosphoenzyme from gene level takes 26 seconds.***** *In general biochemistry, one amino acid is considered an average of 110 daltons*

There is a large rate difference between times of protein phosphorylation and translation. While the time length of protein/amino acid phosphorylation is stated as seconds/milliseconds, time span of translation is stated as minutes. Why do some cells first react to a biotic/abiotic signal by phosphorylation? These bionumbers may be attributed to, the cell spends more time to make new proteins by regulation through turning genes on/off than creation new derivative molecules with post-transcriptional modifications. Priority for the plant cells have to adapt as possible quickly to micro vicinity that is re-decorated at molecular level within seconds/milliseconds to self-protect from bio-detrimental impact of surroundings along evolutionary process. So the result is inevitable that plants should be primarily carried out protein phosphorylation, subsequently attempted to molecule synthesis by promoting gene induction in plant immune systems.

5. CONCLUSION

Protein phosphorylation has crucial roles for plant immunity. Quantitative analysis experiments with the time-course of immune protein phosphorylation are usually limited. Due to researches related on time length of protein/amino acid expression are standardized in chronobiology and also difficulty of the stoichiometric measurement of protein phosphorylation they are not intensely focused nowadays. Hence the expansion of analytical studies on quantitative determination level of plant immune protein phosphorylation is necessary. With advances in innovative technologies, the discovery of novel phosphoproteins/amino acids or uncovering of currently existing ones in plant defense pathways may contribute to ponder layout behind mechanism of cellular communication network which is very complex. Endeavors in this area might be the boost to foster for designing new paths of alternative fundamental plant protection strategies.

CONFLICT OF INTEREST

The authors stated that there are no conflicts of interest regarding the publication of this article.

REFERENCES

[1] Li S, Xiong Q, Lai X, Li X, Wan M, Zhang J, Yan Y, Cao M, Lu L, Guan J, et al. Molecular Modification of Polysaccharides and Resulting Bioactivities. Compr Rev Food Sci F, 2016;15:237-250.

[2] Pandeya SN, Dimmock JR. An Introduction to Drug Design. New Age International Publishers, New Delhi, 1997.

[3] Audagnotto M, Dal Peraro M. Protein post-translational modifications: *In silico* prediction tools and molecular modeling. Comput Struct Biotechnol, J 2017;15:307-319.

[4] di Pietro M, Vialaret J, Li GW, Hem S, Prado K, Rossignol M, Maurel C, Santoni V, et al. Coordinated post-translational responses of aquaporins to abiotic and nutritional stimuli in *Arabidopsis* roots. Mol Cell Proteomics, 2013;12:3886-3897.

[5] Spoel SH. Orchestrating the proteome with post-translational modifications. J Exp Bot, 2018;69:4499-4503.

[6] Krause C, Richte, S, Knöll C, Jürgens G. Plant secretome: from cellular process to biological activity. Biochim Biophys Acta, 2013;183:2429-2441.

[7] Matsubayashi Y. Posttranslationally modified small-peptide signals in plants. Annu Rev Plant Biol, 2014;65:385-413.

[8] Hashiguchi A, Komatsu S. Posttranslational Modifications and Plant-Environment Interaction. Methods Enzymol, 2017;586:97-113.

[9] Yalçın A. Posttranslasyonel Modifikasyon ve Protein Fonksiyonu. Uludağ Üniversitesi Veteriner Fakültesi Dergisi, 2012;31:29-38.

[10] Kadota Y, Macho AP, Zipfel C. Immunoprecipitation of plasma membrane receptor-like kinases for identification of phosphorylation sites and associated proteins. Methods Mol Biol, 2016;1363:133-144.

[11] Lemeer S, Heck AJ. The phosphoproteomics data explosion. Curr Opin Chem Biol, 2009;13:414-420.

[12] Schulze B, Mentzel T, Jehle AK, Mueller K, Beeler S, Boller T, Felix G, Chinchilla D. Rapid heteromerization and phosphorylation of ligand-activated plant transmembrane receptors and their associated kinase BAK1. J Biol Chem,2010;285:9444-9451.

[13] Stram AR, Payne RM. Post-translational modifications in mitochondria: protein signaling in the powerhouse. Cell Mol Life Sci, 2016;73:4063-4073.

[14] Virág D, Dalmadi-Kiss B, Vékey K, Drahos L, Klebovich I, Antal I, Ludányi K. Current trends in the analysis of post-translational Modifications. Chromatographia, 2020;83:1-10.

[15] Martin BL. Regulation by Covalent Modification. In eLS, John Wiley and Sons Ltd (Ed.), Chichester, 2014.

[16] Osakabe Y, Yamaguchi-Shinozaki K, Shinozaki K, Tran LS. Sensing the environment: key roles of membrane-localized kinases in plant perception and response to abiotic stress. J Exp Bot, 2013;64:445-458.

[17] Yu Q, An L, Li W. The CBL-CIPK network mediates different signaling pathways in plants. Plant Cell Rep, 2014;33:203-214.

[18] Li J, Silva-Sanchez C, Zhang T, Chen S, Li H. Phosphoproteomics technologies and applications in plant biology research. Front Plant Sci, 2015;6:430.

[19] Krebs EG. The enzymology of control by phosphorylation. In:Boyer PD, Krebs EG, editors. The Enzymes. New York: Academic Press, 1986;17:pp.3-20.

[20] Olsen JV, Blagoev B, Gnad F, Macek B, Kumar C, Mortensen P, Mann M. Global, in-vivo, and site-specific phosphorylation dynamics in signaling networks. Cell, 2006;127:635-648.

[21] Thingholm TE, Jensen ON, Larsen MR. Analytical strategies for phosphoproteomics. Proteomics, 2009;9:1451–1468.

[22] Ha JH, Loh SN.Protein conformational switches: from nature to design. Chemistry, 2012;18:7984-7999.

[23] Xu S, Xiao J, Yin F, Guo X, Xing L, Xu Y, Chong K. The Protein Modifications of *O*-GlcNAcylation and Phosphorylation Mediate Vernalization Response for Flowering in Winter Wheat. Plant Physiol, 2019;180:1436-1449.

[24] Benschop JJ, Mohammed S, O'Flaherty M, Heck AJ, Slijper M, Menke FL. Quantitative phosphoproteomics of early elicitor signaling in *Arabidopsis*. Mol Cell Proteom, 2007;6:1198-1214.

[25] Al-Momani S, Qi D, Ren Z, Jones AR. Comparative qualitative phosphoproteomics analysis identifies shared phosphorylation motifs and associated biological processes in evolutionary divergent plants. J Proteom, 2018;181:152-159.

[26] Weintz G, Olsen JV, Frühauf K, Niedzielska M, Amit I, Jantsch J,Mages J, Frech C, Dölken L, Mann M, et al. The phosphoproteome of toll-like receptor-activated macrophages. Mol Syst Biol, 2010;6:371.

[27] Haj Ahmad F, Wu XN, Stintzi A, Schaller A, Schulze WX. The Systemin Signaling Cascade As Derived from Time Course Analyses of the Systemin-Responsive Phosphoproteome. Mol Cell Proteom, 2019;18:1526-1542.

[28] Otto V, Schäfer E. Rapid Phytochrome-Controlled Protein Phosphorylation and Dephosphorylation in *Avena sativa* L. Plant Cell Physiol, 1988;29:1115-1121.

[29] Briskin DP, Leonard RT. Phosphorylation of the adenosine triphosphatase in a deoxycholate-treated plasma membrane fraction from corn roots. Plant Physiol, 1982;70:1459-1464.

[30] Briskin DP. Phosphorylation and dephosphorylation reactions of the red beet plasma membrane ATPase studied in the transient state. Plant Physiol, 1988;88:84-91.

[31] Rose ZB, Dube S. Rates of phosphorylation and dephosphorylation of phosphoglycerate mutase and biphosphoglycerate synthase. J Biol Chem, 1976;251:4817-4822.

[32] Tang W, Yuan M, Wang R, Yang Y, Wang C, Oses-Prieto JA, Kim TW, Zhou HW, Deng Z, Gampala SS, et al. PP2A activates brassinosteroid-responsive gene expression and plant growth by dephosphorylating BZR1. Nat Cell Biol, 2011;13:124-131.

[33] Park CJ, Caddell DF, Ronald PC. Protein phosphorylation in plant immunity: insights into the regulation of pattern recognition receptor-mediated signaling. Front Plant Sci, 2012;3:177.

[34] Minkoff BB, Stecker KE, Sussman MR. Rapid Phosphoproteomic Effects of Abscisic Acid (ABA) on Wild-Type and ABA Receptor-Deficient *A. thaliana* Mutants. Mol Cell Proteom, 2015;14:1169-1182.

[35] Yin J, Yi H, Chen X, Wang J. Post-Translational Modifications of Proteins Have Versatile Roles in Regulating Plant Immune Responses. Int J Mol Sci, 2019;20:2807.

[36] Delom F, Chevet E. Phosphoprotein analysis: from proteins to proteomes. Proteome Sci, 2006;4:15.

[37] Hargrove JL, Hulsey MG, Beale EG. The kinetics of mammalian gene expression. Bioessays, 1991;13:667-674.

[38] Lewin B. Genes VI. Oxford University Press; New Ed Edition, Oxford, 1997.

[39] Rawn JD. Biochemistry, Neil Patterson Publishers, Burlington, USA, 1989.

[40] Alberts B, Bray D, Lewis J, Raff M, Roberts K, Walter P. Molecular Biology of the Cell. 3rd ed. New York: Garland Science, 1994.